APPENDIX C

PHOTOCHEMICAL MODELING FOR THE HGB ATTAINMENT DEMONSTRATION SIP REVISION FOR THE 2008 EIGHT-HOUR OZONE STANDARD

Project Number 2016-016-SIP-NR

Adoption
December 15, 2016

APPENDIX C: PHOTOCHEMICAL MODELING FOR THE HGB ATTAINMENT DEMONSTRATION SIP REVISION FOR THE 2008 EIGHT-HOUR OZONE STANDARD

Table of Contents

CHAPTER 1: OVERVIEW

The development of the base case photochemical modeling for this Attainment Demonstration (AD) State Implementation Plan (SIP) Revision proceeded through a number of iterations, which involved updates and improvements in the meteorological and emissions modeling. The final photochemical modeling configuration is described in Chapter 3. The meteorological modeling is detailed in Appendix A: *Meteorological Modeling for the HGB Attainment Demonstration SIP Revision for the 2008 Eight-Hour Ozone Standard*. Development of the emission inventories is described in Appendix B: *Emissions Modeling for the HGB Attainment Demonstration SIP Revision for the 2008 Eight-Hour Ozone Standard*. Because of the short time for completing this SIP revision, a limited performance evaluation is shown below.

CHAPTER 2: PERFORMANCE COMPARISON WITH THE 2013 HGB 1997 EIGHT-HOUR OZONE MVEB SIP REVISION

On January 2, 2014 the EPA approved the 2013 HGB 1997 Eight-Hour Ozone MVEB SIP Revision, which established a motor vehicle emission budget for the area based on the Motor Vehicle Emission Simulator (MOVES). That SIP revision will be referred to as the MOVES SIP. The current modeling has many similarities to the MOVES SIP but significant differences exist beyond updating the emissions and model versions. Most significantly, the current modeling used a single five-month episode in 2012 (May through September), while the MOVES SIP modeling used a 2006 base case which coincided with the TexAQS II field study. The MOVES SIP modeling used three episodes covering June 1 through 15, August 15 through September 14, and September 19 through October 11, 2006, referred to, respectively, as June06, AQS1, and AQS2 (AQS refers to Air Quality Study). The current and MOVES SIP used a Lambert Conformal map Conic projection (LCC), but the current modeling domains cover larger geographic areas in each domain. The current modeling uses the CB6r2h chemical mechanism, which includes halogen chemistry, while the MOVES SIP modeling used the CBo5 chemical mechanism.

In considering the relative performance of the two modeling applications, it is important to remember that the current modeling includes an entire ozone season while the MOVES SIP modeling focused on high-ozone periods. Performance on high-ozone days is important, but since the model is used in a relative sense, model responsiveness is ultimately the key to a modeling demonstration. Since the model's dynamic range may limit its responsiveness, it is important to examine performance during periods of both low and high ozone.

In the following bar charts, statistics calculated for the current SIP revision are displayed in the last five columns in light blue. The MOVES SIP episodes are displayed in the first three columns and are colored light orange.

Horizontal lines represent a compilation of performance statistics from 69 model runs conducted by various organizations during the years 2006 through 2012 (Simon, et al, 2012). These lines allow comparison of the current work to the body of similar analyses conducted in recent years. The solid line represents the median of each statistic presented, and the two lines featuring longer dashes represent the first and

third quartiles. The lines with short dashes represent the minimum and maximum values reported across the studies (the minimum value is limited to the first quartile minus 1.5 times the interquartile range, and the maximum is limited to the third quartile plus 1.5 times the interquartile range). A few studies limited the statistical calculations to use only modeled-observed pairs where the observed value exceeded a threshold (usually 40 or 60 ppb), but most used all of the data. The compilations include all studies regardless of whether a threshold was employed.

Figure 2-1: *Mean Bias Comparison, All Modeled-Observed One-Hour Pairs* shows model bias calculated for one-hour average ozone concentrations for the two TCEQ SIP modeling efforts using all modeled-observed data pairs. The bias for the current modeling is much lower than that for the MOVES SIP. Modeling for May and June of 2012 is within the interquartile range of recent studies, with the remaining three months slightly outside.

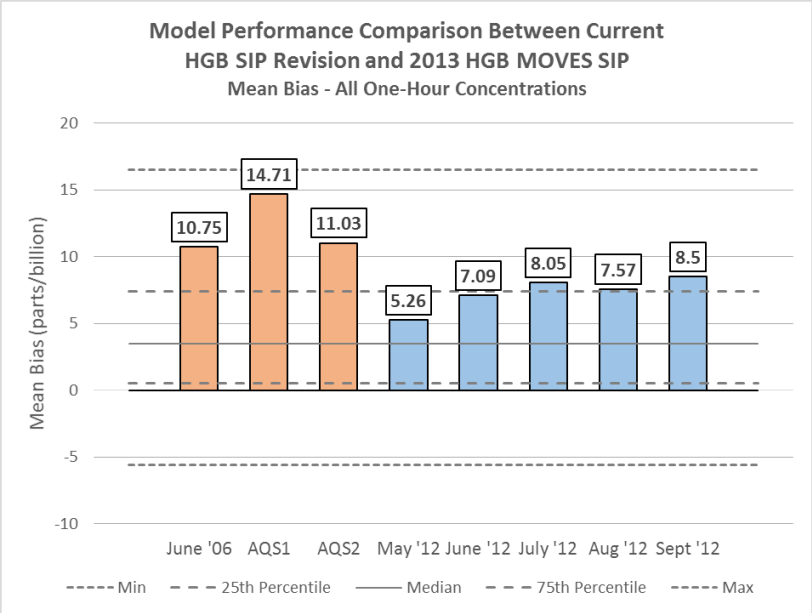

Figure 2-1: Mean Bias Comparison, All Modeled-Observed One-Hour Pairs

While the current modeling shows definite improvement over the MOVES SIP when evaluating over all observed ozone concentrations, the performance differs when values above the 60 ppb threshold are considered. Figure 2-2: *Mean Bias Comparison, Modeled-Observed One-Hour Pairs with Observed Concentration ≥ 60* shows that the model predicts higher ozone concentrations well in all eight periods considered, with bias within 4 ppb (plus or minus) of zero. These values compare very favorably with the compiled studies' bias values, which show a median of +3.5 ppb. Only June 2012 had a bias of greater magnitude (3.57 ppb).

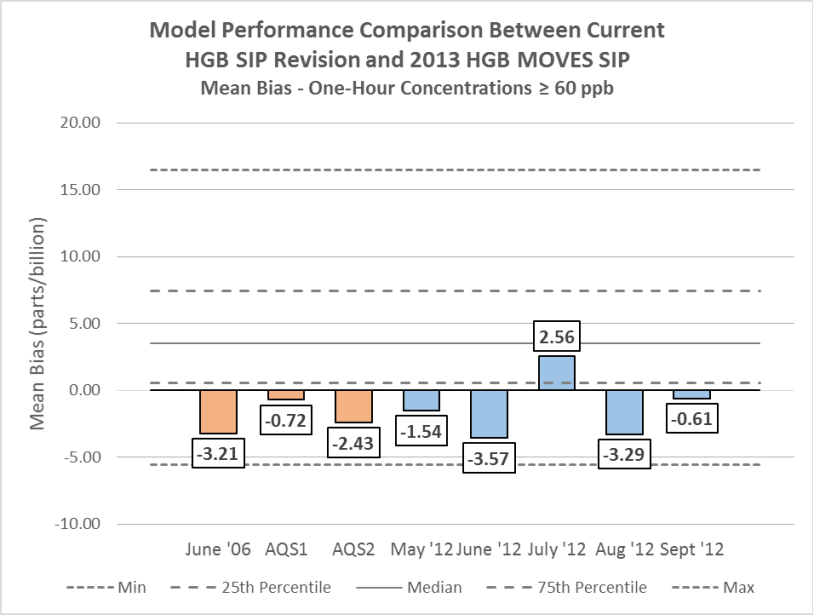

Figure 2-2: Mean Bias Comparison, Modeled-Observed One-Hour Pairs with Observed Concentration ≥ 60 ppb

Figure 2-3: *RMSE Comparison, All Modeled-Observed One-Hour Pairs* shows root mean-square error (RMSE) for the current and MOVES SIP modeling platforms. By this measure, the 2012 modeling performs better than any of the compiled modeling results. The MOVES SIP modeling performed reasonably well, but not as well as the current application.

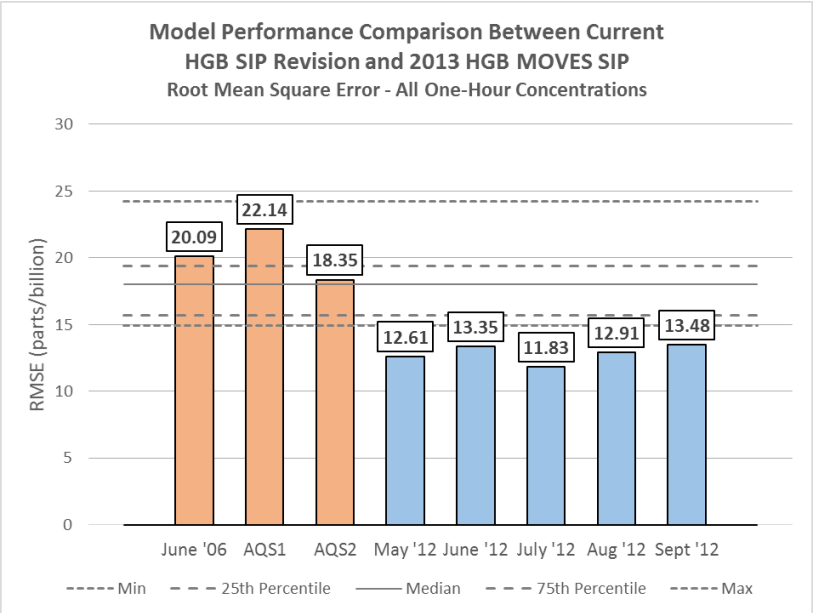

Figure 2-3: RMSE Comparison, All Modeled-Observed One-Hour Pairs

When considering data pairs with observed ozone at or above a 60 ppb threshold, both the current and MOVES SIP modeling compare well with the reference runs,

outperforming them except for the AQS1 period, as shown in Figure 2-4: *RMSE Comparison, Modeled-Observed One-Hour Pairs with Observed Concentration ≥ 60 ppb*.

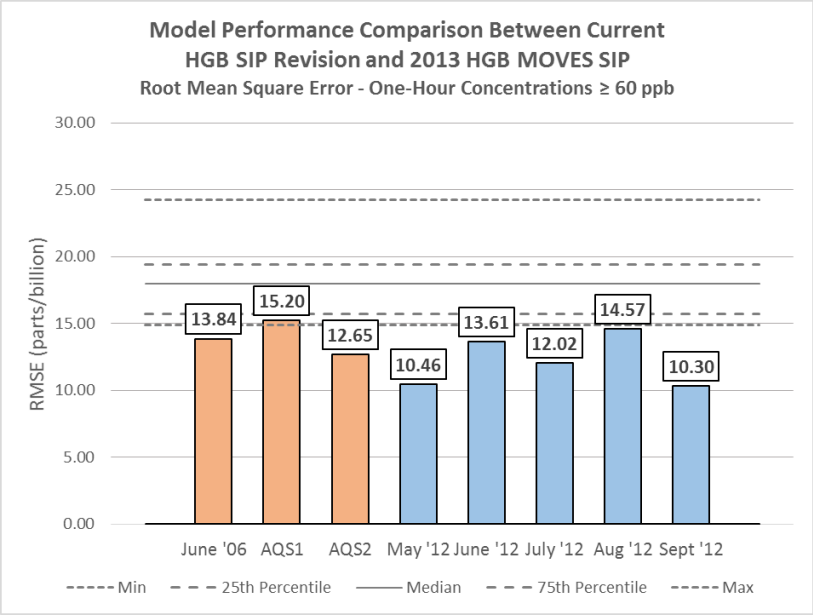

Figure 2-4: RMSE Comparison, Modeled-Observed One-Hour Pairs with Observed Concentration ≥ 60 ppb

For eight-hour ozone concentrations, Figure 2-5: *Mean Bias Comparison, All Modeled-Observed MDA8 Ozone Pairs* compares model bias for maximum daily average eight-hour (MDA8) ozone across the eight modeling periods. When considering all concentration data, model bias is comparable between the MOVES SIP modeling and the 2012 modeling. July shows a significant positive bias, which is expected due to the dominant southerly flow from the Gulf. Some of that bias carries over into August. May, June, and September all have biases somewhat above the third quartile.

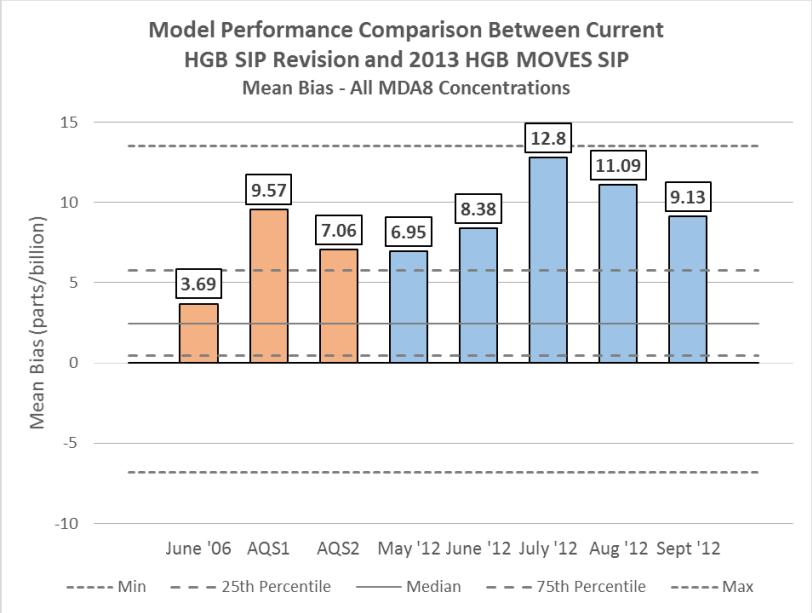

Figure 2-5: Mean Bias Comparison, All Modeled-Observed MDA8 Ozone Pairs

Figure 2-6: *Model Bias for MDA8 Ozone, Data Pairs with Observed Ozone ≥ 60 ppb* shows bias for MDA8 ozone above a threshold of 60 ppb. Only the 2012 modeling is shown since data for the MOVES SIP runs was not available. No data is displayed for July since there were zero days where any monitor in HGB recorded an MDA8 concentration above 60 ppb. These results indicate essentially zero bias for predictions of MDA8 ozone concentrations that may affect the area's ozone design value.

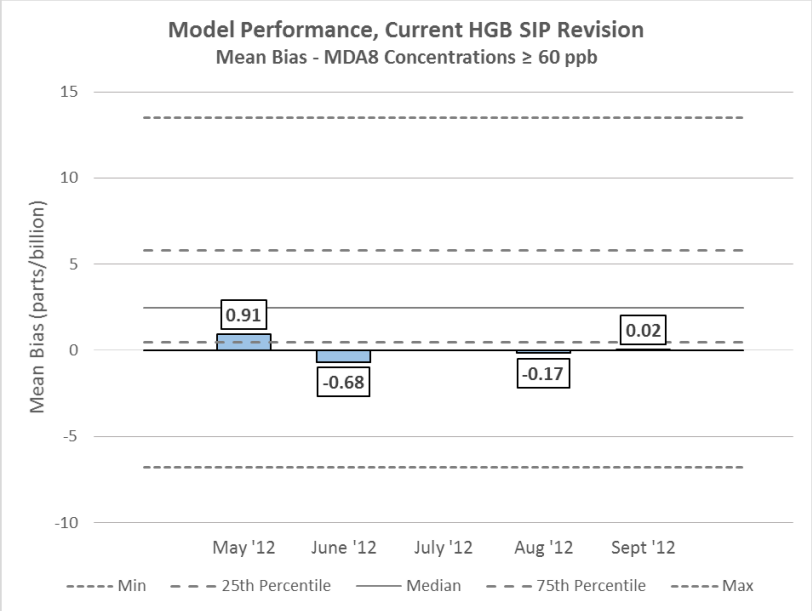

Figure 2-6: Model Bias for MDA8 Ozone, Data Pairs with Observed Ozone ≥ 60 ppb

CHAPTER 3: MODEL PERFORMANCE SNAPSHOTS

This section looks at several model performance evaluation methods at selected sites in the HGB nonattainment area to help assess how well CAMx can replicate the physical atmosphere.

3.1 GALVESTON AIRPORT (C1034)

The first site examined is Galveston Airport - C1034 with its location noted in green in Figure 3-1: *Galveston Airport – C1034 Location*.

Figure 3-1: Galveston Airport (C1034) Location

Halogen chemistry was first added to CAMx in December 2014 to alleviate the significant over-prediction of ozone concentrations seen along the Texas Coast. The blue line in Figure 3-2: *Time Series of Modeled and Observed Ozone for June 2012 at Galveston Airport (C1034), First Halogen Run vs. No Halogen* Chemistry shows simulated ozone without halogen chemistry, and the green line shows improved performance after halogen chemistry was introduced. While significant over-prediction remained, adding halogen chemistry reduced over-prediction by up to 8 ppb and improved performance for almost the entire month.

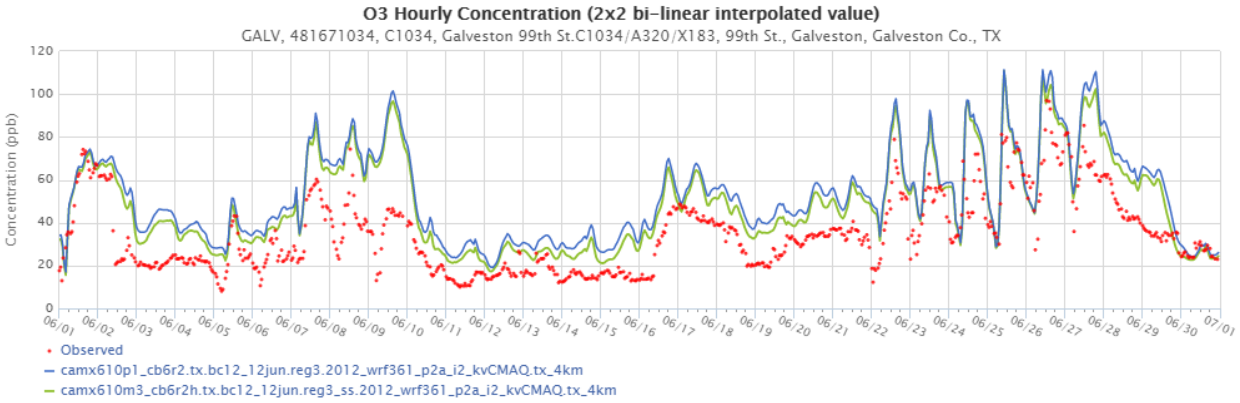

Figure 3-2: Time Series of Modeled and Observed Ozone for June 2012 at Galveston Airport (C1034), First Halogen Run vs. No Halogen Chemistry

Figure 3-3: *Time Series of Modeled and Observed Ozone for June 2012 at Galveston Airport (C1034), Current vs First Halogen* Run shows a time series comparing the current base case with the first CAMx halogen run (green line in both the figure above and the one below). Additional model refinements over the past 18 months have yielded good model performance especially on days with higher observed ozone as shown with the blue line for the current model configuration in Figure 3-3.

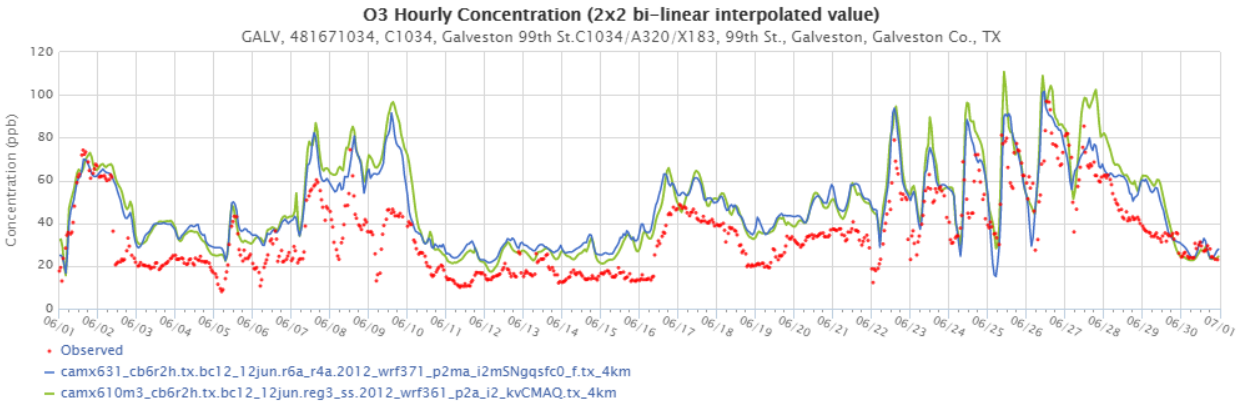

Figure 3-3: Time Series of Modeled and Observed Ozone for June 2012 at Galveston Airport (C1034), Current vs First Halogen Run

3.2 CONROE RELOCATED (C78)

Conroe C78 is on the opposite (northern) end of the nonattainment area from Galveston (see Figure 3-4: *Conroe Relocated (C78) Location*). Along with significant amounts of local emissions, mostly traffic, Conroe Relocated – C78 is frequently affected by emissions advected northward from the HGB urban core and industries in eastern Harris County. The time series in Figure 3-5: *Time Series of Modeled and Observed Ozone at Conroe (C78) for June 2012* shows good ozone performance for the base case in June 2012 except for over-prediction of the nighttime concentrations during the last half of the episode. Figure 3-6: *Time Series of Modeled and Observed Ozone at Conroe (C78) for August 2012* shows the same figure for August where model performance again is good, except for over-predicting some peak daily concentrations in the 60-75 ppb range. In Figure 3-7: *Time Series of Modeled and Observed Ozone at Conroe (C78) for September 2012*, model performance on the peaks is exemplary, although again some of the lower nighttime values are over-predicted. Time series plots showing a single model run include bands showing the minimum and maximum concentrations within the 3x3 grid cell array containing the monitor.

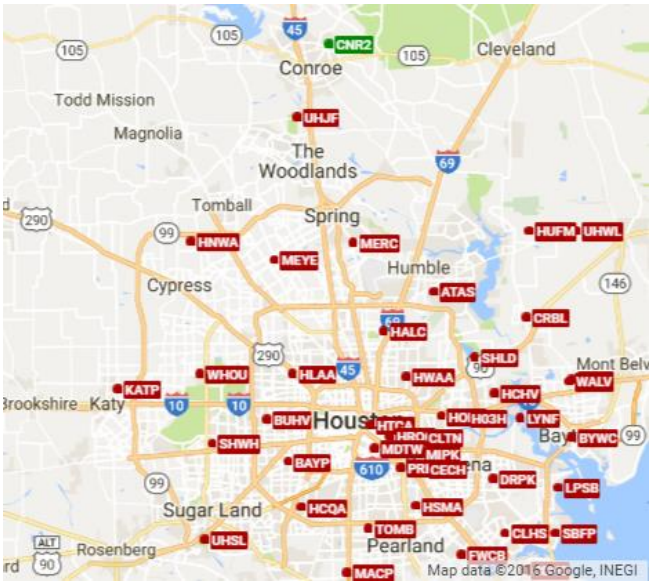

Figure 3-4: Conroe Relocated (C78) Location

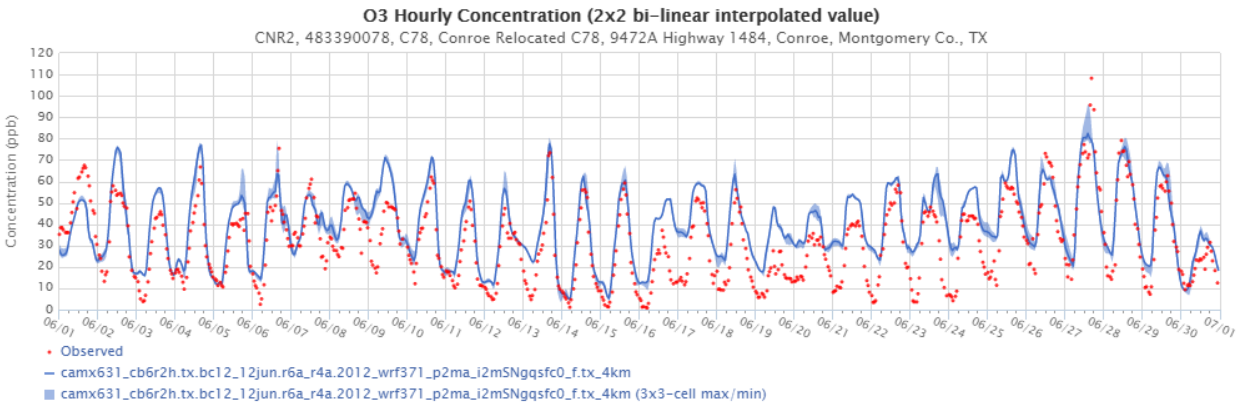

Figure 3-5: Time Series of Modeled and Observed Ozone at Conroe (C78) for June 2012

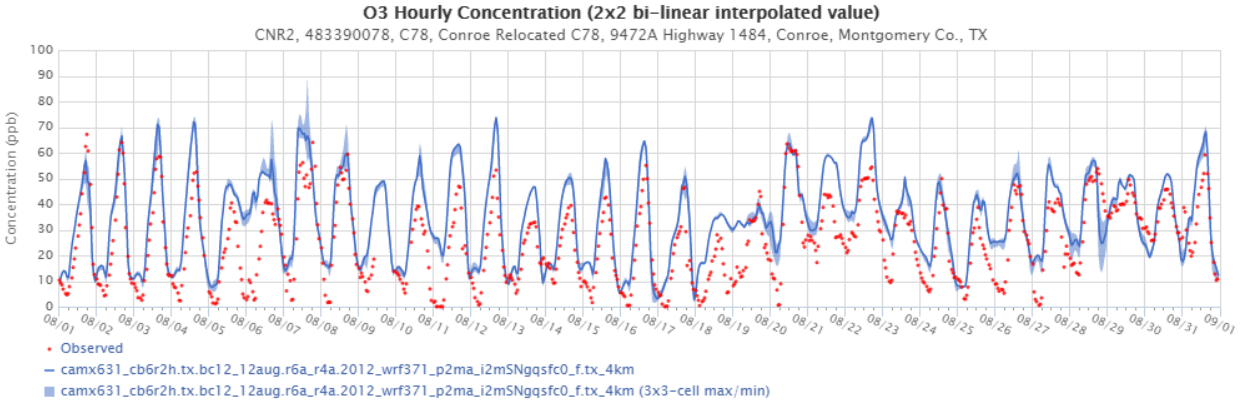

Figure 3-6: Time Series of Modeled and Observed Ozone at Conroe (C78) for August 2012

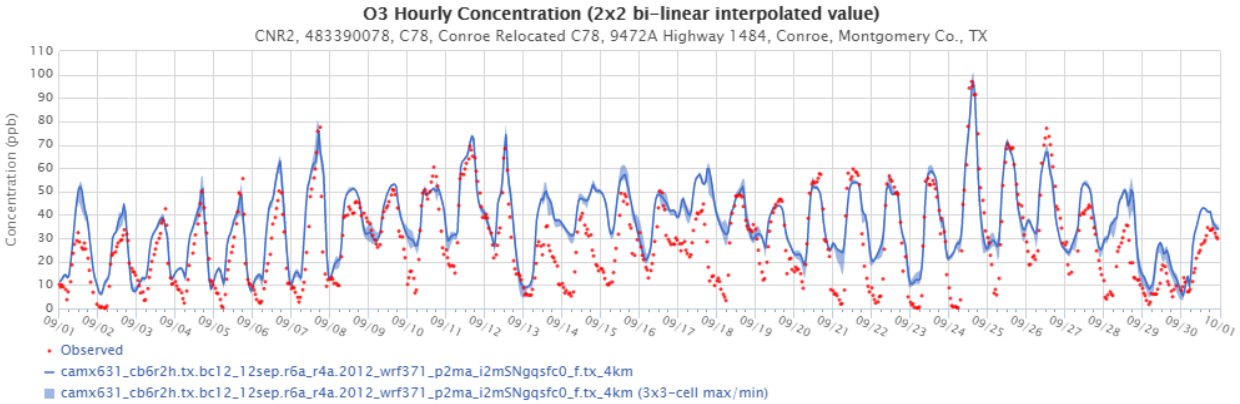

Figure 3-7: Time Series of Modeled and Observed Ozone at Conroe (C78) for September 2012

Figure 3-8: *Time series of Modeled and Observed NO_x at Conroe (C78) for June 2012* shows the June time series for NO_x at Conroe Relocated, and offers some explanation for the model nighttime ozone over-prediction. The model over-estimates NO_x

concentrations between 21:00 and 06:00, which implies ozone is being titrated. Inadequate mixing in the first couple of hundred meters is a suspected cause. Meanwhile daytime NO_X appears to be under-estimated. The wide blue bands show that modeled NO_X varies widely among grid cells, reinforcing the notion of incommensurability between a point measurement and the volume of a 4x4 km grid cell in which it is located. Performance can be affected by a monitor's location within a grid cell.

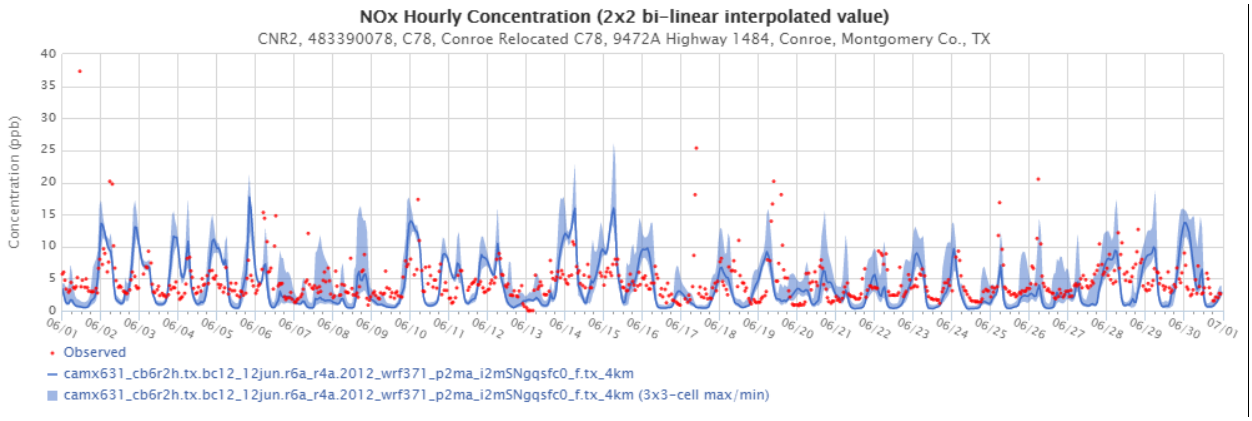

Figure 3-8: Time series of Modeled and Observed NO_X at Conroe (C78) for June 2012

Figure 3-9: *Cumulative Density Plot of Modeled and Observed NO_X at Conroe (C78) for June 2012* presents another view of the NO_X concentrations. This plot compares the modeled and observed cumulative densities. Although the observations in this plot are unpaired in space and time, it shows how well the model represents the distribution of observed concentrations. The vertical gradients represent deciles of the respective distributions: first decile (0.1) shows 10% of the observed values lie below about 2 ppb, while 10% of modeled concentrations lie below 0.6 ppb. At the median (0.5) half of the observations are below 3.7 ppb, while half of the modeled concentrations are below 2.7 ppb. About two-thirds of both observed and modeled distributions lie below 4.7 ppb. Beyond this point, the modeled distribution overtakes the observations until approximately the 98th percentile, where some extreme observations push the observed distribution ahead. In short, the model has fewer low (< 4.6 ppb) concentrations than observed, but has more above 4.6 ppb except for a few extreme observations.

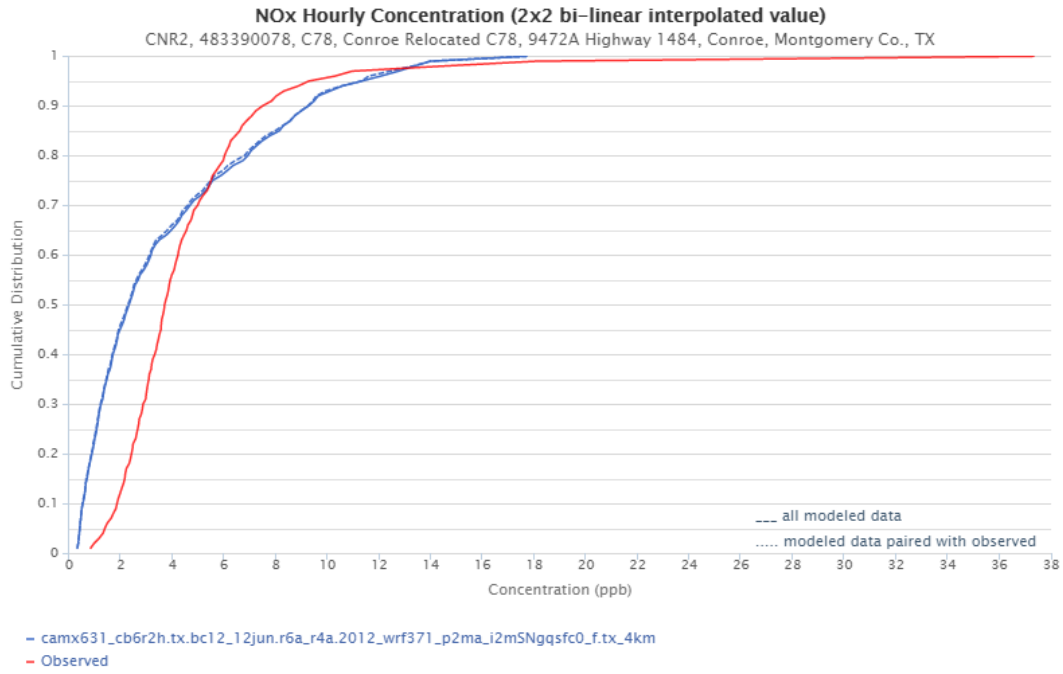

Figure 3-9: Cumulative Density Plot of Modeled and Observed NO_x at Conroe (C78) for June 2012

3.3 FAYETTE COUNTY (C601)

Fayette County (C601) is a rural site located west of the HGB nonattainment area, as shown in Figure 3-10: *Fayette County (C601) Location*. Although Fayette County is not normally a background site for HGB, it is occasionally a downwind site and is representative of the model's ability to replicate ozone concentrations in an area with urban influence. Figure 3-11: *Time Series of Modeled and Observed Ozone at Fayette County (C601) for June 2012*, Figure 3-12: *Time Series of Modeled and Observed Ozone at Fayette County (C601) for July 2012*, and Figure 3-13: *Time Series of Modeled and Observed Ozone at Fayette County (C601) for* August 2012 show time series for June through August, respectively, at Fayette County (C601). Throughout the period shown the model does a very credible job of following the rise and fall of ozone and matching the peaks, although there is a tendency to over-predict very low concentrations in the early morning. These low observed concentrations most likely result from ozone titration caused by fresh NO_x emissions near the monitor being trapped beneath a nocturnal inversion and may result from localized effects beyond the 16 km^2 resolution of the model. In July, observed concentrations are low throughout the month, a trend reflected well in the model. August performance is reasonable. The

model missed the observed peak on August 20, a day that saw widespread high ozone over much of the southern half of Texas.

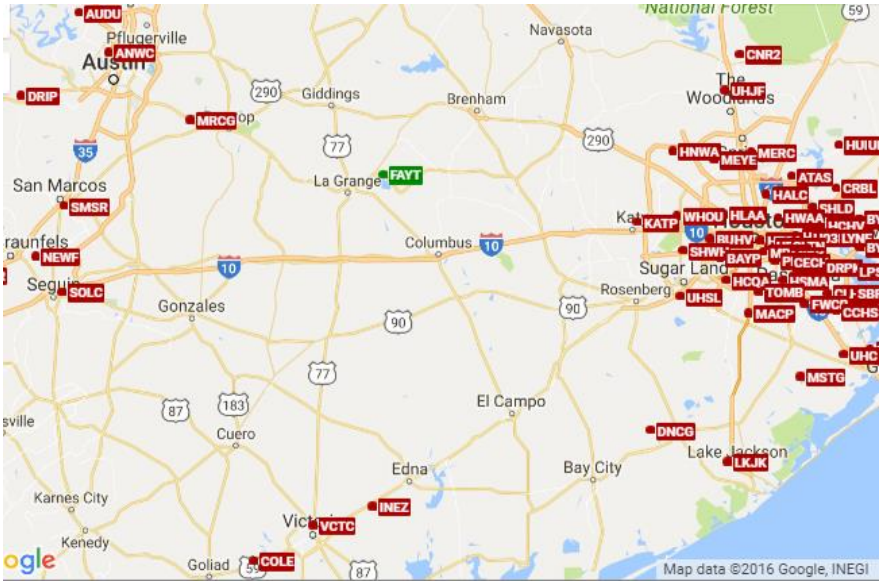

Figure 3-10: Fayette County (C601) Location

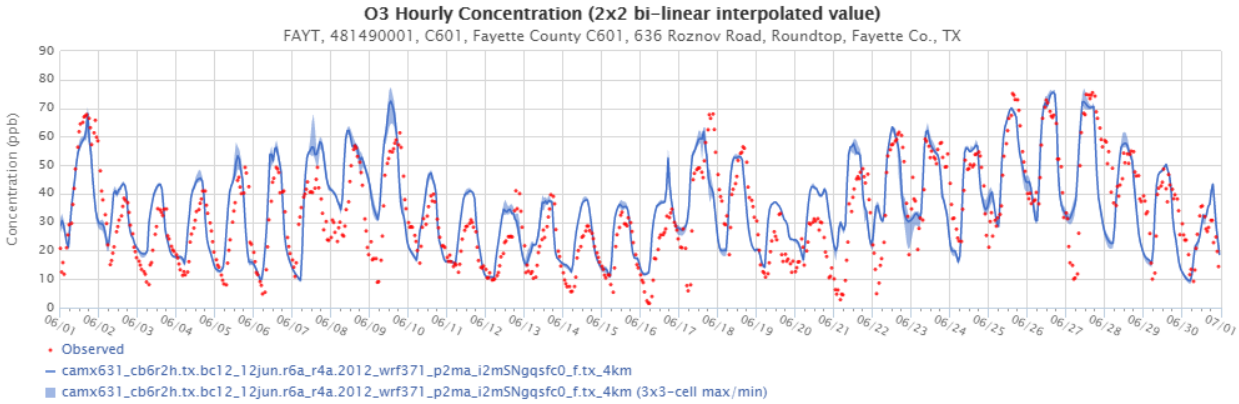

Figure 3-11: Time Series of Modeled and Observed Ozone at Fayette County (C601) for June 2012

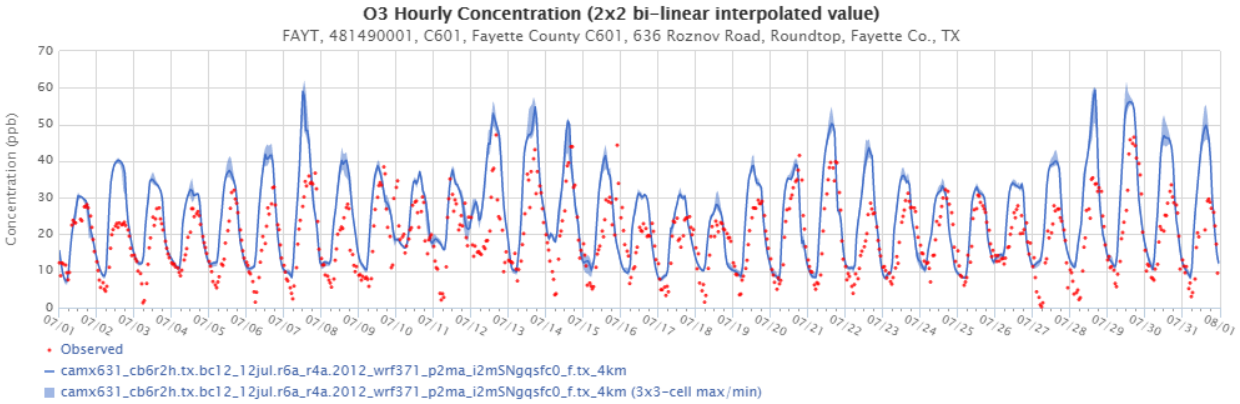

Figure 3-12: Time Series of Modeled and Observed Ozone at Fayette County (C601) for July 2012

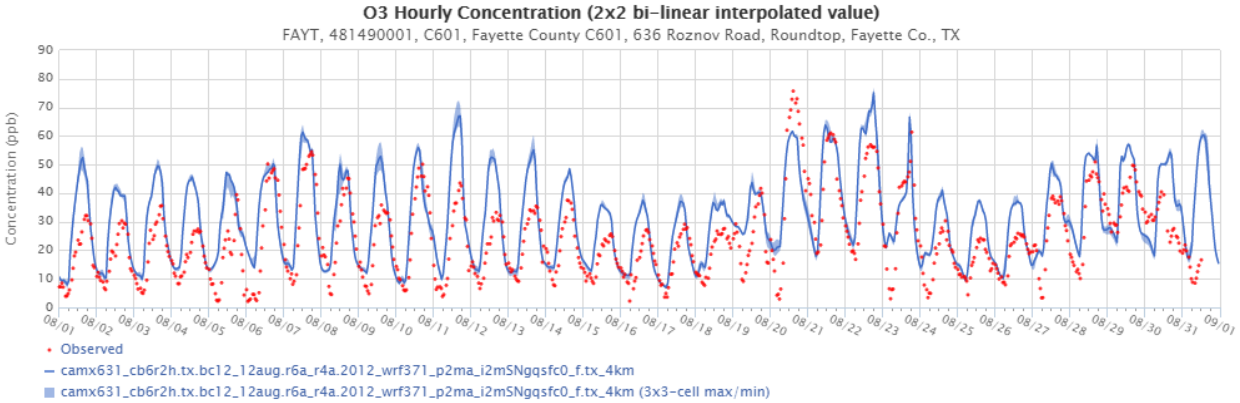

Figure 3-13: Time Series of Modeled and Observed Ozone at Fayette County (C601) for August 2012

3.4 ALDINE (C8)

Aldine (C8) is a suburban site that is occasionally downwind of the Houston Ship Channel or the Houston urban core (see Figure 3-14: *Aldine (C8)* Location). Figure 3-15: *Time Series of Modeled and Observed Ozone at Aldine (C8) for June 2012*, Figure 3-16: *Time Series of Modeled and Observed NO_X at Aldine (C8) for June 2012*, and Figure 3-17: *Time Series of Modeled and Observed CO at Aldine (C8) for June 2012* show time series of observed and modeled ozone, NO_X, and CO, respectively for Aldine (C8) for June 2012. Ozone performance is generally good, replicating the high peaks observed on June 26 and 27 well. Performance of NO_X and CO is also good, especially considering the localized nature of roadways and other NO_X and CO sources compared with the 4 km grid cell size.

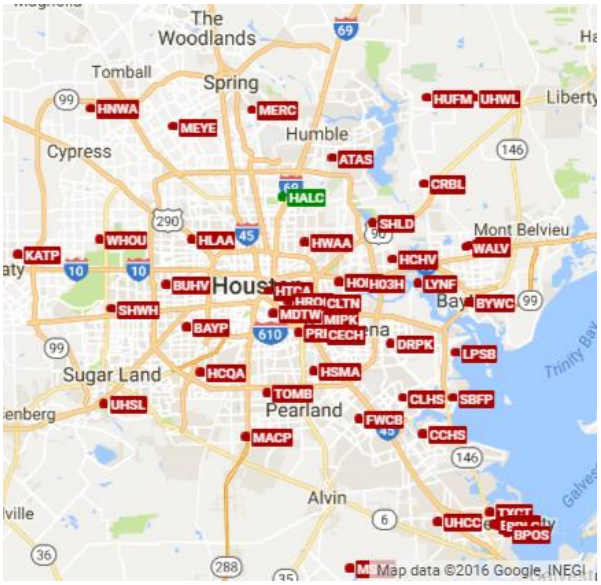

Figure 3-14: Aldine (C8) Location

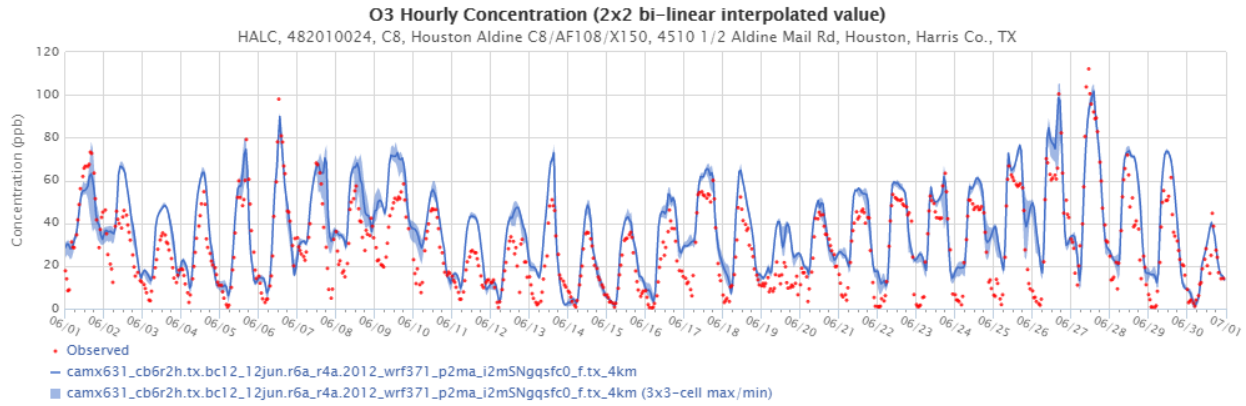

Figure 3-15: Time Series of Modeled and Observed Ozone at Aldine (C8) for June 2012

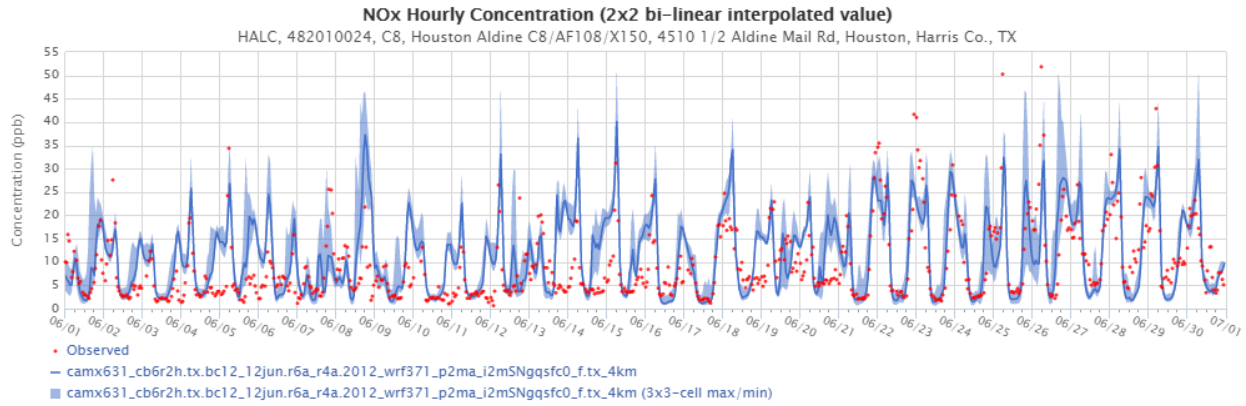

Figure 3-16: Time Series of Modeled and Observed NO_x at Aldine (C8) for June 2012

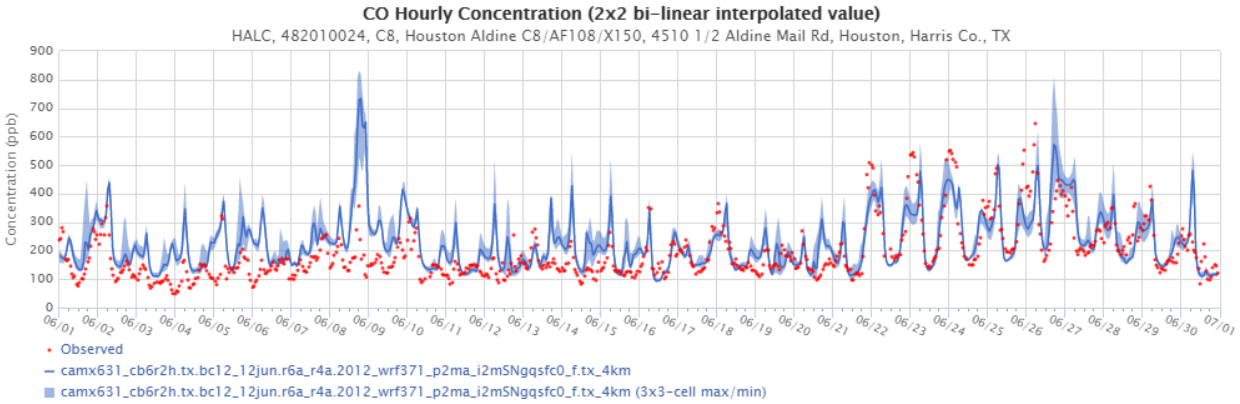

Figure 3-17: Time Series of Modeled and Observed CO at Aldine (C8) for June 2012

Figure 3-18: *Cumulative Density Plot of Modeled and Observed NO_X at Aldine (C8) for June 2012* and Figure 3-19: *Cumulative Density Plot of Modeled and Observed CO at Aldine (C8) for June 2012* show cumulative density plots of the NO_X and CO data displayed above, and show a modest positive bias for both pollutants. Median modeled NO_X concentration is 10.05 ppb compared with observed median of 6.27 ppb, while modeled median CO concentration is 188.23 ppb compared with an observed median of 158.9 ppb.

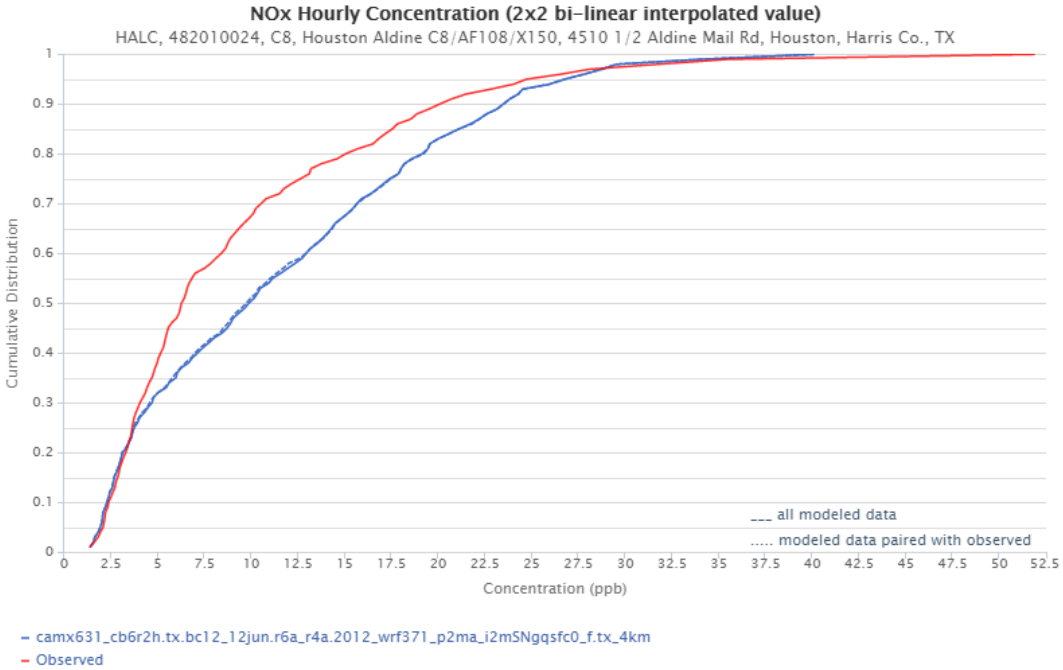

Figure 3-18: Cumulative Density Plot of Modeled and Observed NO_X at Aldine (C8) for June 2012

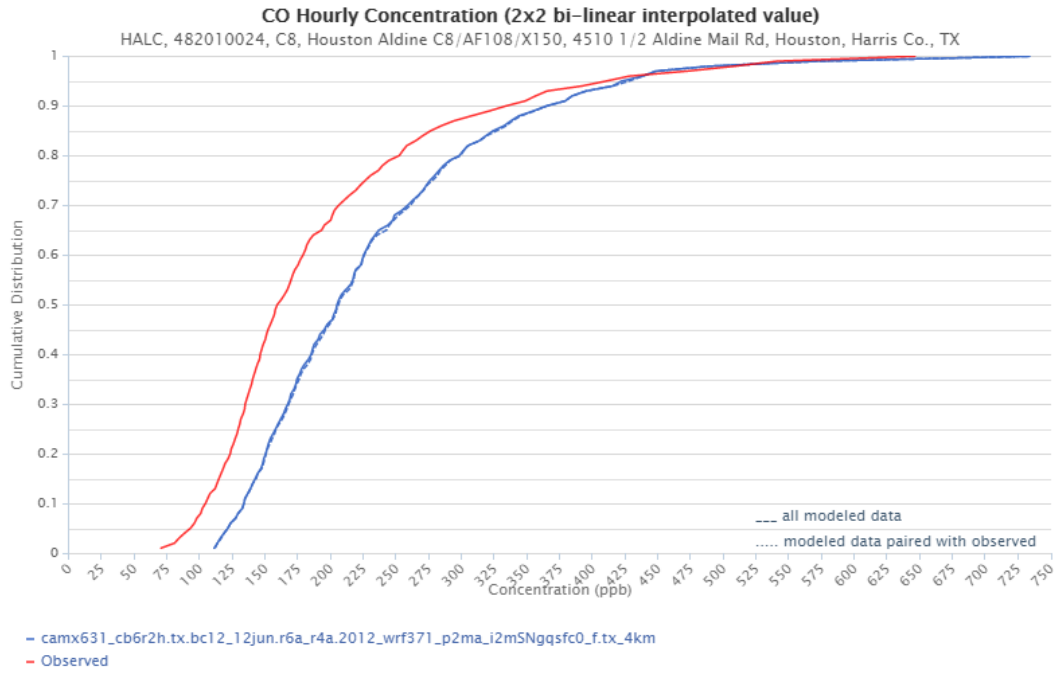

Figure 3-19: Cumulative Density Plot of Modeled and Observed CO at Aldine (C8) for June 2012

3.5 DEER PARK (C35)

Deer Park (C35) is located south of the Ship Channel industrial area (Figure 3-20: *Deer Park (C35)* Location). This site measures not only ozone, NO_x, and CO but also collects hourly speciated hydrocarbon data using an automated gas chromatograph (auto-GC). Figure 3-21: *Time Series of Modeled and Observed Ozone at Deer Park (C35) for August 2012* shows observed and modeled ozone concentrations for August 2012. The model matches the peak concentrations well temporally, but under-predicts all three peaks above 90 ppb by 10 to 15 ppb. The model over-predicts some peaks in the 40 ppb range, but does well matching the early morning lows. Figure 3-22: *Time Series of Modeled and Observed NO_x at Deer Park (C35) for August 2012* shows a tendency to over-predict NO_x, although the model predicts morning peak concentrations reasonably well. Figure 3-23: *Time Series of Modeled and Observed CO at Deer Park (C35) for August 2012* compares modeled and observed CO, and shows a relatively strong tendency to over-predict CO concentrations outside the August 20 through 27 period.

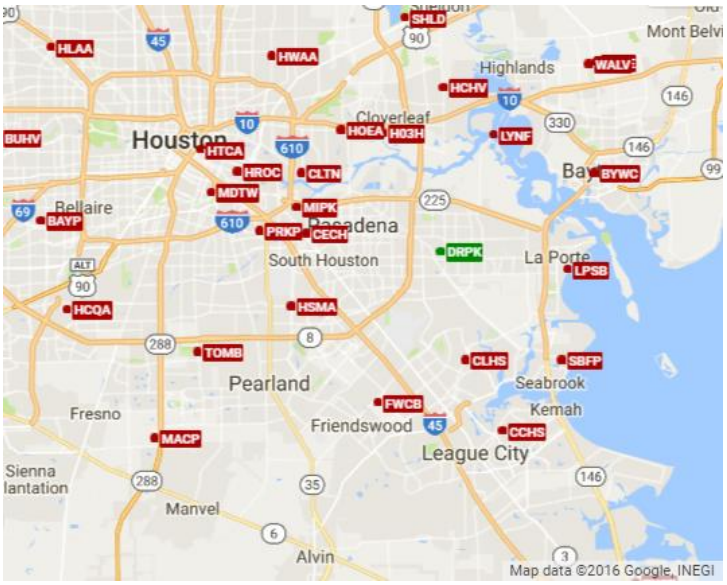

Figure 3-20: Deer Park (C35) Location

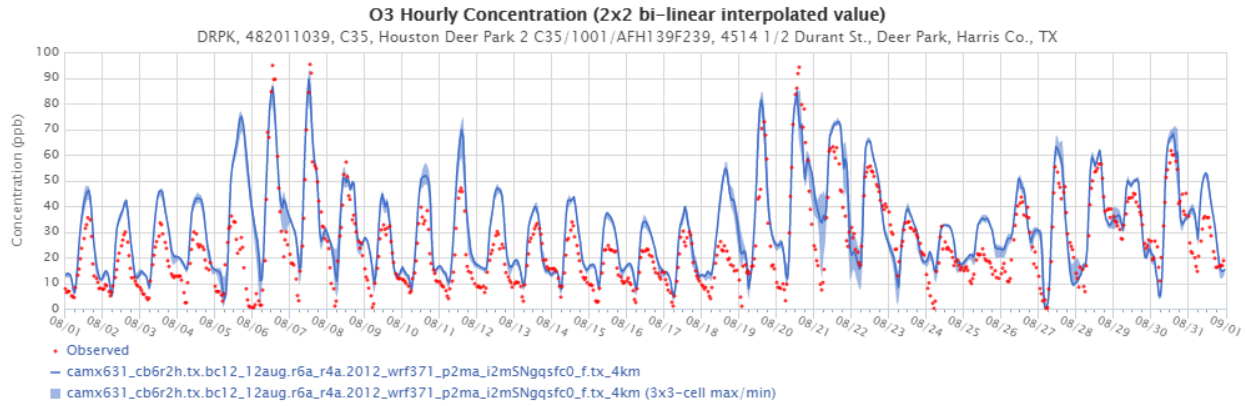

Figure 3-21: Time Series of Modeled and Observed Ozone at Deer Park (C35) for August 2012

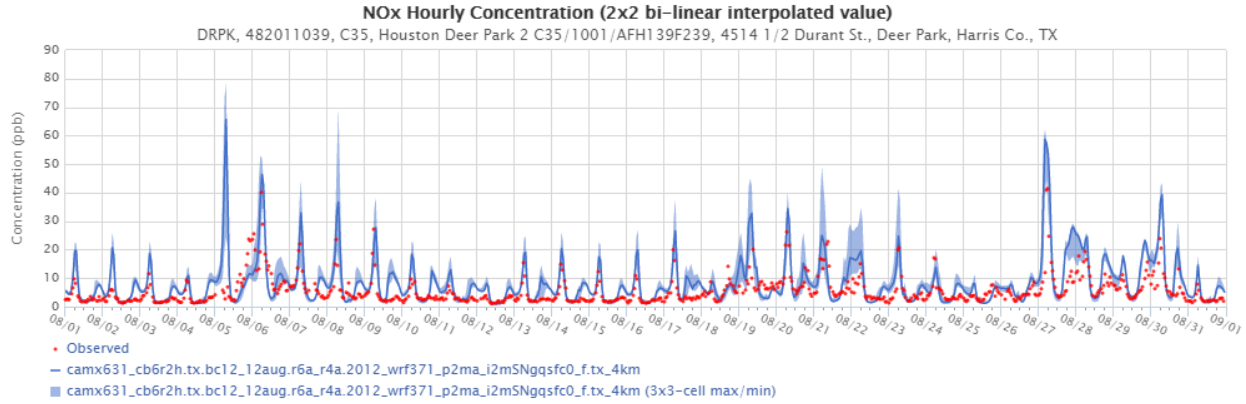

Figure 3-22: Time Series of Modeled and Observed NO_x at Deer Park (C35) for August 2012

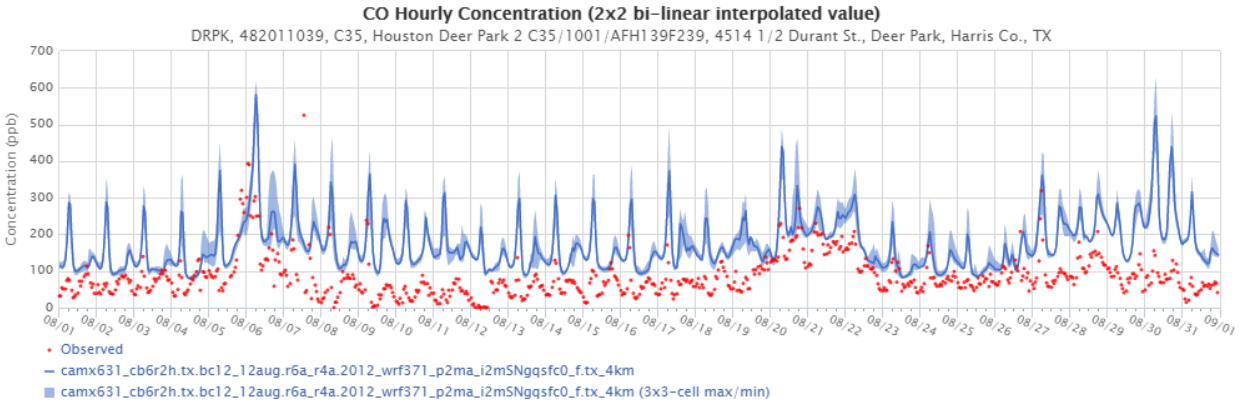

Figure 3-23: Time Series of Modeled and Observed CO at Deer Park (C35) for August 2012

The next several figures show time series comparing several CB6 hydrocarbon species with observations. With a few exceptions (most notably ETH – ethene, ETHA – ethane, PRPA – propane, and ISOP – isoprene) the actual hydrocarbon data undergo a transformation according to the carbon-carbon bond structure for comparison to photochemical model output. For example, PAR represents a single C-C bond, which is found in a large variety of organic molecules, so the CB6 PAR species represents all or part of many different atmospheric chemicals. Figure 3-24: *Time Series of Modeled and Observed ETH (ethene) at Deer Park (C35) for August 2012* and Figure 3-25: *Time Series of Modeled and Observed OLE (certain olefins) at Deer Park (C35) for August 2012* show that ETH and OLE, two highly-reactive CB6 species, tend to be over-predicted overnight. On the other hand, daytime concentrations are modeled fairly well on most days, as shown in Figure 3-26: *Time Series with Reduced Scale of Modeled and Observed OLE (certain olefins) at Deer Park (C35) for August 2012*.

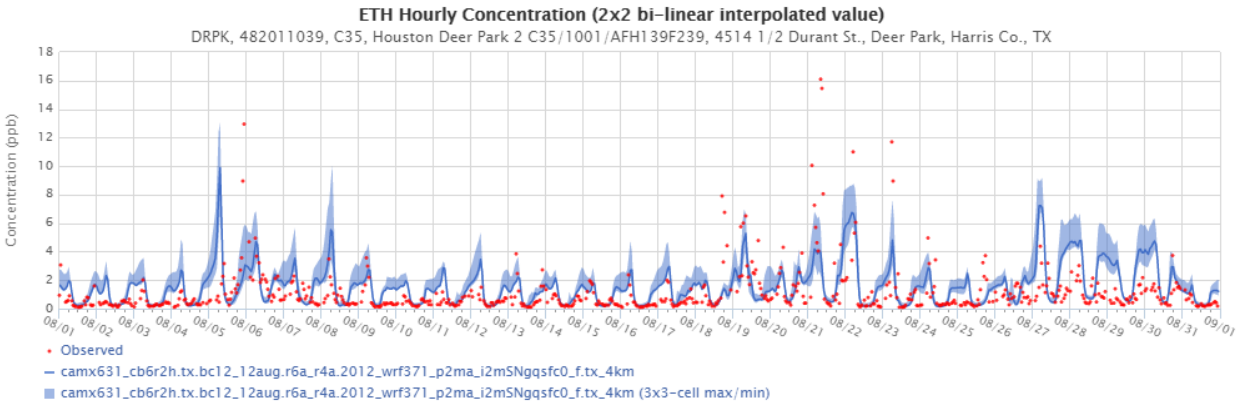

Figure 3-24: Time Series of Modeled and Observed ETH (ethene) at Deer Park (C35) for August 2012

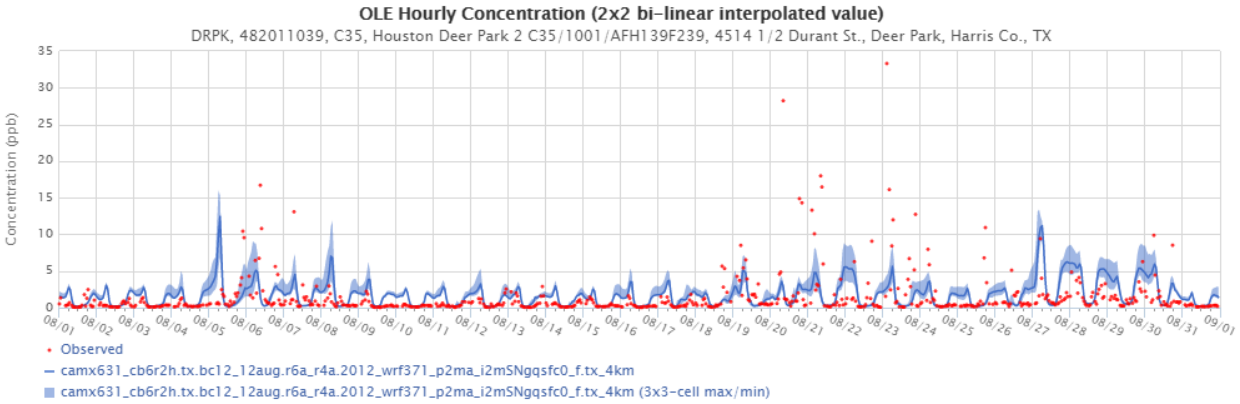

Figure 3-25: Time Series of Modeled and Observed OLE (certain olefins) at Deer Park (C35) for August 2012

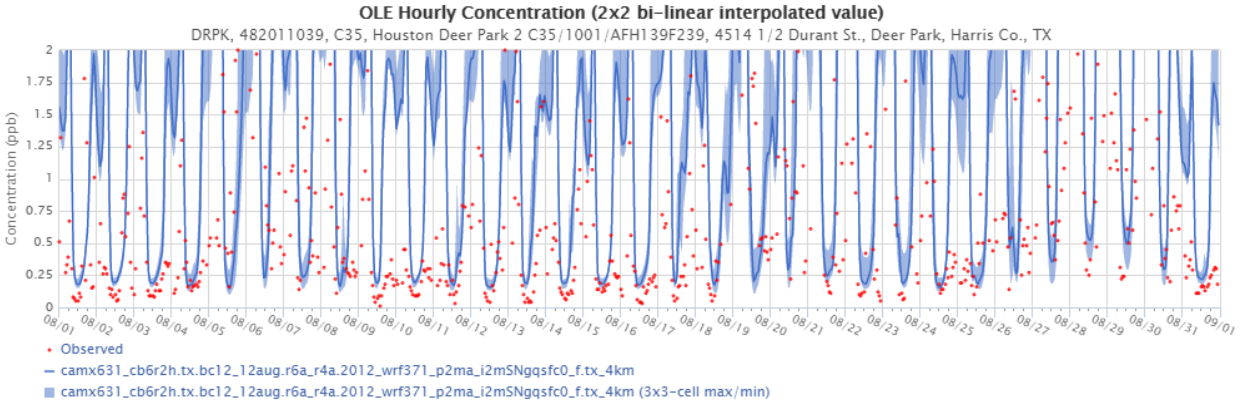

Figure 3-26: Time Series with Reduced Scale of Modeled and Observed OLE (certain olefins) at Deer Park (C35) for August 2012

Figure 3-27: *Time Series of Modeled and Observed PAR at Deer Park (C35) for August 2012* shows the time series for the CB6 species PAR. On many nights the observed concentrations were relatively low, under 30 ppb, and in these cases the model usually over-predicted the concentrations. However, during periods when the overnight/early morning concentrations were higher, specifically August 3 through 9, August 19 through 24, and August 27 through 30 the model also produced higher concentrations and matched the timing of the observed concentration increases and decreases well.

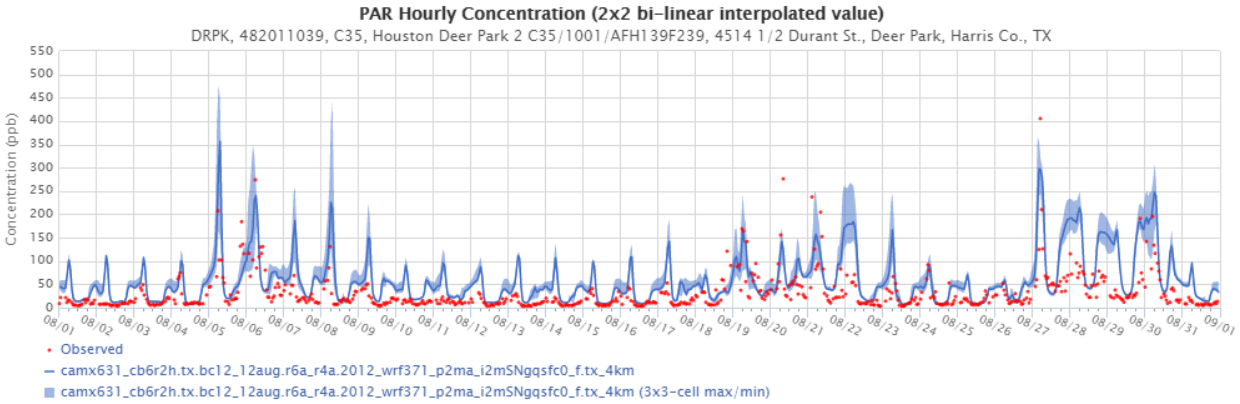

Figure 3-27: Time Series of Modeled and Observed PAR at Deer Park (C35) for August 2012

3.6 DANCIGER (C618)

Danciger (C618) is an auto-GC site and its rural location makes it a good site for evaluating biogenic isoprene concentrations in the model (Figure 3-28: *Danciger (C618) Location*). Figure 3-29: *Time Series of Modeled and Observed ISOP (isoprene) at Danciger (C618) for September 2012* shows a time series of modeled and observed isoprene concentrations for September 2012 and shows that the model matches the diurnal variation very well, although the model sometimes misses the highest concentrations. A large petrochemical facility a few miles south of the monitor may add to the observed isoprene concentrations under certain conditions.

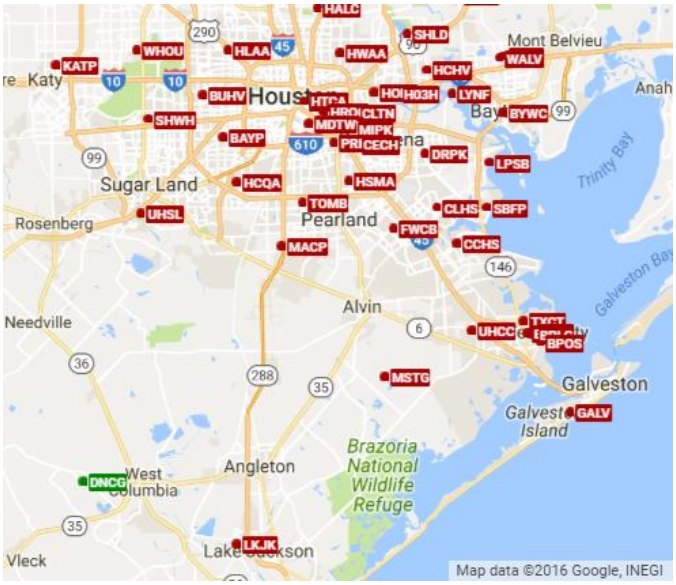

Figure 3-28: Danciger (C618) Location

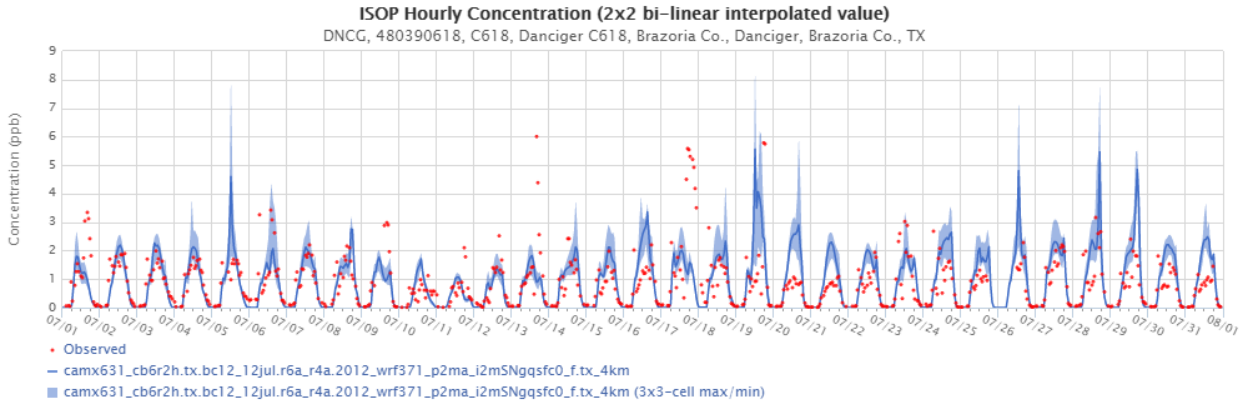

Figure 3-29: Time Series of Modeled and Observed ISOP (isoprene) at Danciger (C618) for September 2012

3.7 MANVEL CROIX PARK (C84)

Manvel Croix Park (C84) (Figure 3-30: *Manvel Croix Park (C84) Location*) has frequently recorded some of the highest MDA8 ozone concentrations in the HGB area in recent years. It has the highest measured 2015 design value and the highest modeled DV_F. Figure 3-31: *Time Series of Modeled and Observed Ozone at Manvel Croix Park (C84) for August 2012* shows a time series of modeled and observed ozone concentrations for August 2012. For the first 18 days the model does a good job replicating low to moderate peaks, but tends to over-predict the very low early morning concentrations. Beginning on August 19 through 23 the overnight concentrations are much higher and the model replicates them fairly well. On August 20 and 21 the monitor recorded the highest one-hour concentrations of the month and the model replicates the timing of those peaks well but falls short of matching the amplitude. The model does a better job of matching the peak on August 27 and again matches the timing of the peak on August 28 but not the magnitude. During the two late-month periods of elevated ozone the model matches the lower ozone concentrations fairly well.

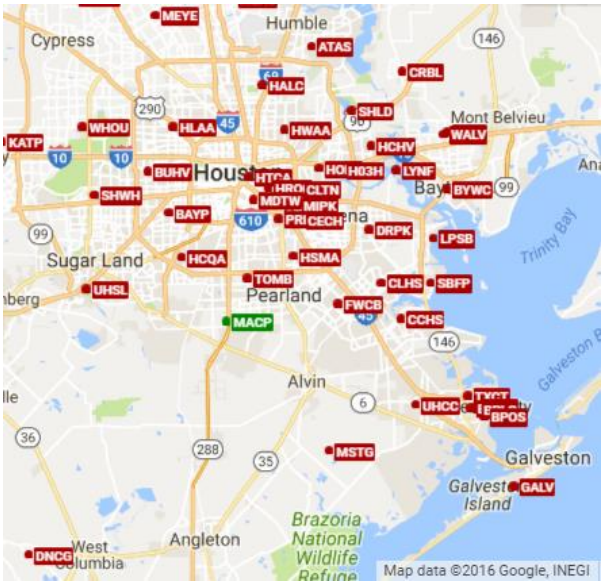

Figure 3-30: Manvel Croix Park (C84) Location

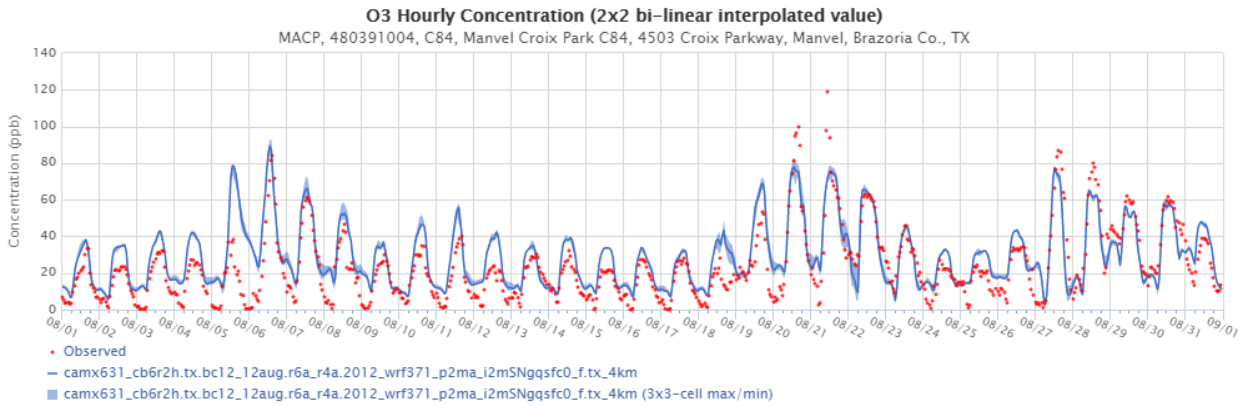

Figure 3-31: Time Series of Modeled and Observed Ozone at Manvel Croix Park (C84) for August 2012

Figure 3-32: *Cumulative Density Plot of Modeled and Observed NO_X at Manvel Croix Park (*C84*) for August 2012* shows a CDF plot of modeled and observed NO_X at Manvel for the month of August, and shows generally low observed concentrations. Over most of the distribution of observed NO_X the model shows a fairly constant bias of around 1.5 ppb.

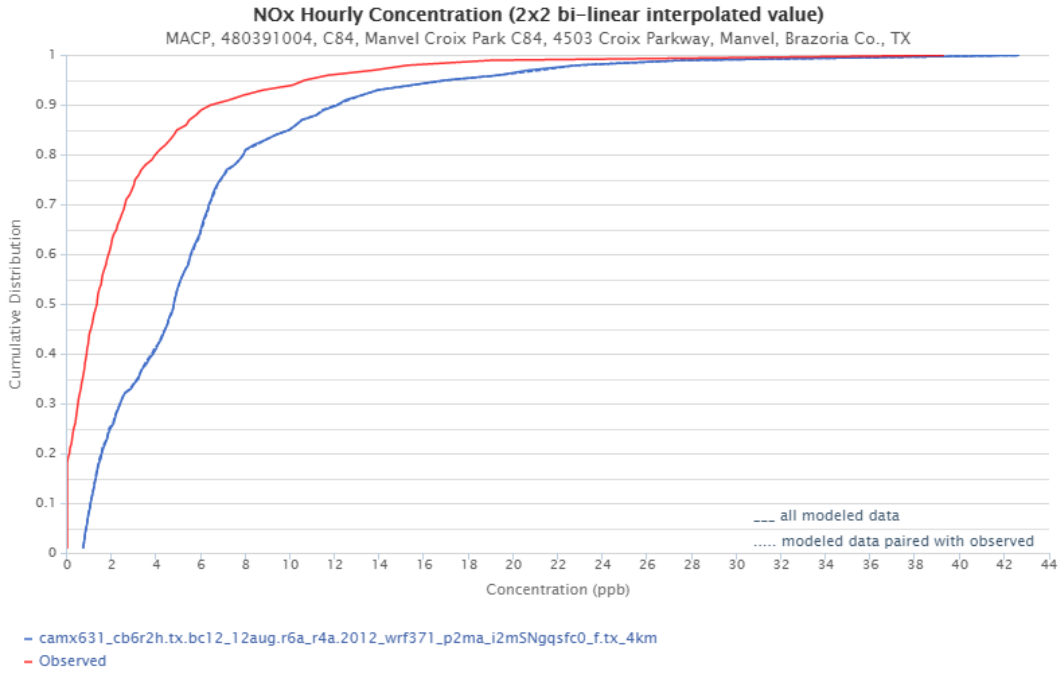

Figure 3-32: Cumulative Density Plot of Modeled and Observed NO_X at Manvel Croix Park (C84) for August 2012

CHAPTER 4: VERTICAL OZONE PROFILES

During the period May through September 2012 there were a total of 20 ozone sonde launches in the Houston area, most from the University of Houston campus near downtown Houston. Figure 4-1: *June 2012 Ozone Sonde Launches in the Houston Area* compares observed and modeled ozone concentrations for the four launches in June 2012. On the first three launches the observed concentrations are fairly constant with increasing altitude to the top of the mixed layer, where they decrease rapidly in the course of a couple of hundred meters. On June 1 and 6 the model shows the same behavior except that modeled concentrations are lower than observed. On June 26, the day that recorded the highest MDA8 ozone concentration of 2012, the model did not show a clear discontinuity at the top of the mixed layer and modeled concentrations at the surface were much lower than observed at the launch site. On the following day's 10:00 AM launch, neither the model nor the balloon saw a distinct boundary layer and modeled and observed ozone concentrations did not diverge widely until around 10 km above the ground. Above 10 km, in the upper troposphere/lower stratosphere, the model appears to be excessively mixing stratospheric ozone downward. This phenomenon is a result of using concentration data from the Goddard Earth Observing Station model with Chemistry (GEOS-Chem) across the top of the modeling grid (about 18250 m above ground level). Sensitivity testing showed that inclusion of the top boundary concentrations has a minimal effect on model performance in June, but the TCEQ plans to revisit the way CAMx handles stratospheric influence on surface ozone in the future.

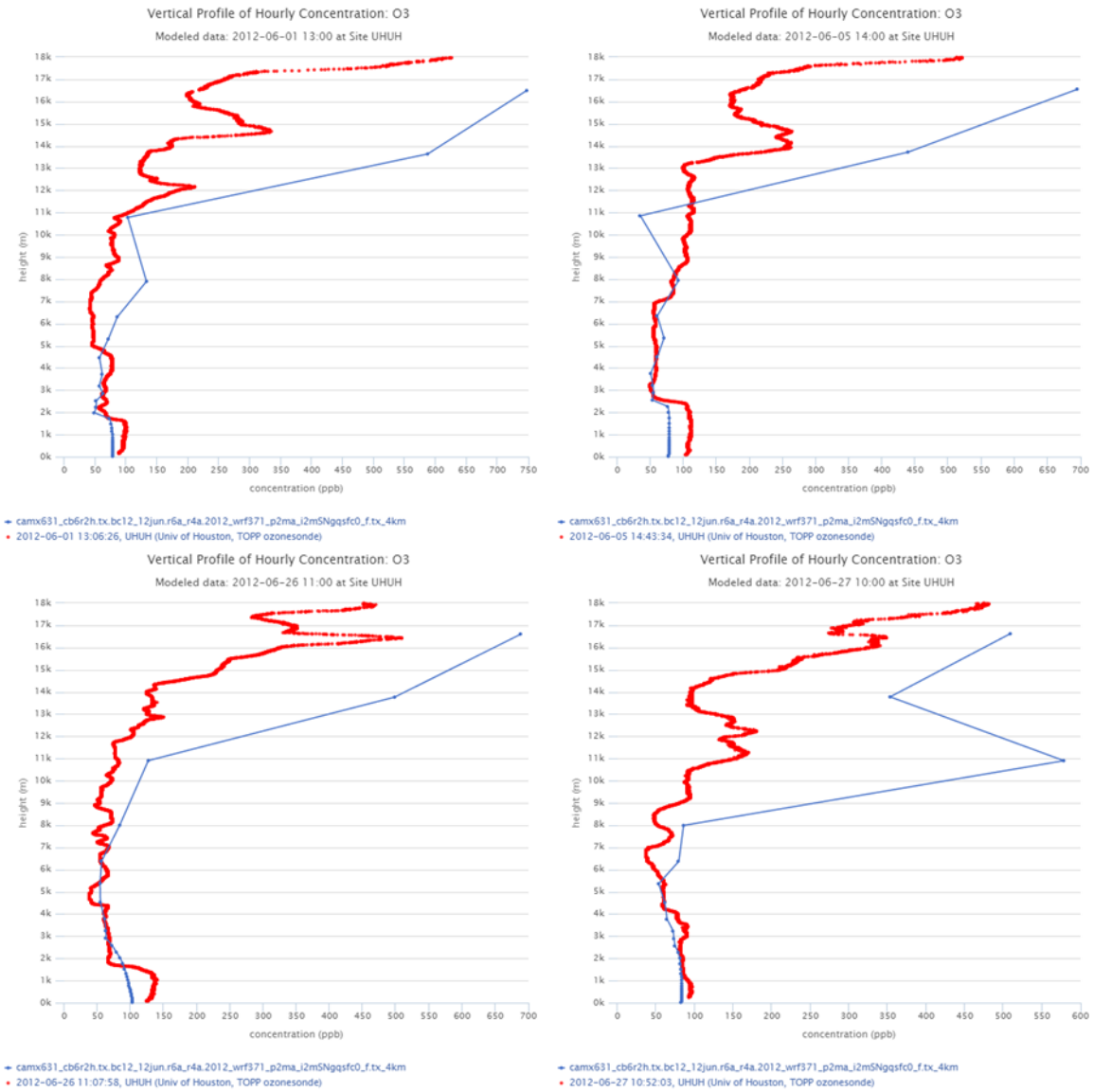

Figure 4-1: June 2012 Ozone Sonde Launches in the Houston Area

Figure 4-2: *September 2012 Ozone Sonde Launches in the Houston Area* compares observed and modeled ozone for the four September sonde launches. The observed ozone concentrations indicated a boundary layer at 2 km on September 8, which was not replicated by the model. On September 21 the ozone sonde indicated a boundary layer at approximately 1.8 km, which was evident in the model. For all four days the model tracked observed ozone concentrations very well to above 10 km, where modeled upper tropospheric concentrations exceeded the observations.

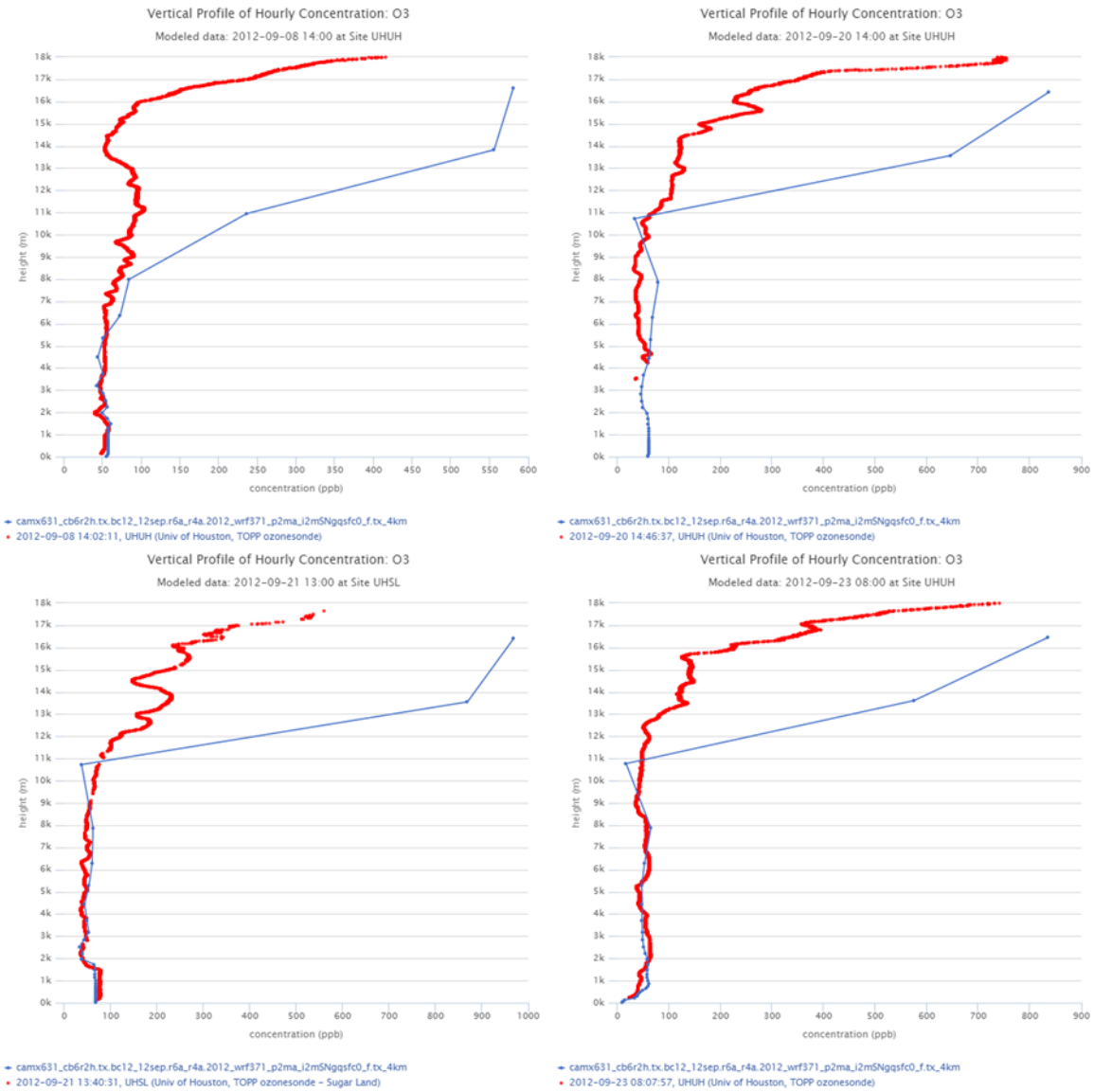

Figure 4-2: September 2012 Ozone Sonde Launches in the Houston Area

CHAPTER 5: SPATIOTEMPORAL DISTRIBUTION OF MODELED OZONE CONCENTRATIONS

This section examines the ability of the model to put high ozone concentrations in the right place. Because it is not possible to exactly replicate wind speed and direction, vertical mixing, cloud cover, and chemical processing in any model, the raw output concentrations will never exactly replicate the observations. Visual inspection of output fields provides a good approach to evaluating how close the model comes.

The plots in this section show one-hour ozone concentrations overlaid with the corresponding observations for two periods, one in May and one in September 2012. The plots show concentrations in the morning, noon, early afternoon, and early

evening and follow the development of both observed and modeled ozone through the respective periods.

5.1 MAY 16 AND 17, 2012

Figure 5-1: Modeled and Observed Ozone Concentrations on May 16, 2012 shows four spatial ozone plots for the day. The upper-left panel (06:00) shows very low observed and modeled ozone concentrations across the area depicted, with the lowest in downtown Houston and along the Ship Channel. These low concentrations result from overnight NO_x emissions in the boundary layer titrating any ozone left over from the day before. The upper-right panel shows that by noon a large plume of moderate ozone had formed and was drifting southwestward. The model agrees well with the observations during this period, and at 14:00 (lower-left panel) and at 17:00 (lower-right panel) as the plume advected to the west.

May 17 showed near-zero modeled ozone concentrations in the area near the Ship Channel at 04:00, as shown in the upper-left panel of Figure 5-2: *Modeled and Observed Ozone Concentrations on May 17, 2012*. Observed concentrations were only slightly higher. By 10:00 (upper-left panel) both the model and monitors showed a large area of moderate ozone to the south and west of the city. By 12:00 the stagnant conditions had built up concentrations over 100 ppb, although the highest observed concentration at Manvel Croix Park - C84 is several kilometers southeast from the modeled peak in West Houston. Simultaneously, the model developed a large pool of ozone over the Gulf. Finally, at 14:00 the model peaked at 96 ppb at Northwest Harris County - C26, matching the observed concentration of 93 ppb (lower right panel). The model missed the observed peak of 103 ppb at West Houston - C554 since the model had its highest concentrations a few kilometers north, but overall the model did a credible job of replicating observed ozone temporally, spatially, and in magnitude over this two-day period.

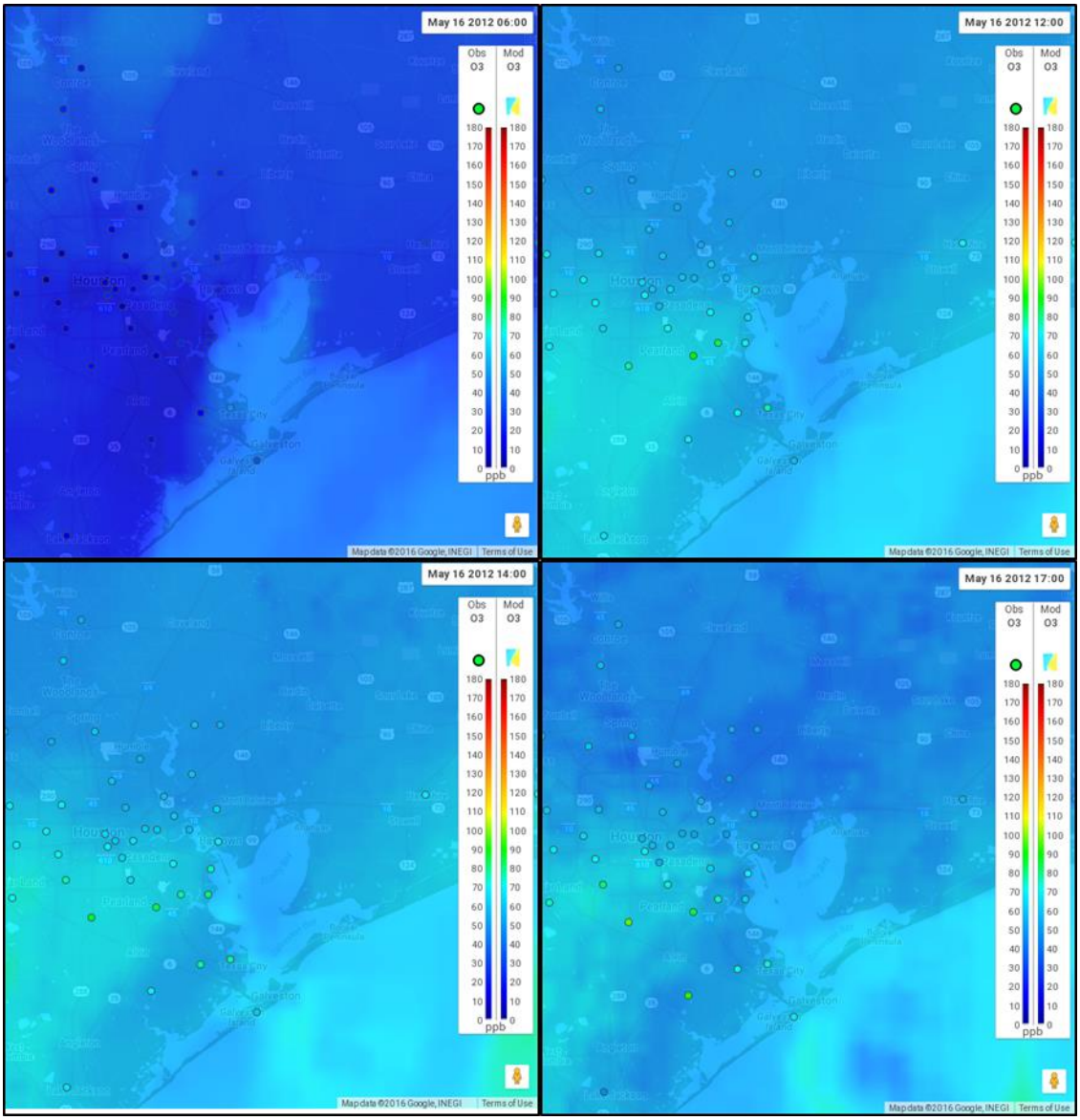

Figure 5-1: Modeled and Observed Ozone Concentrations on May 16, 2012

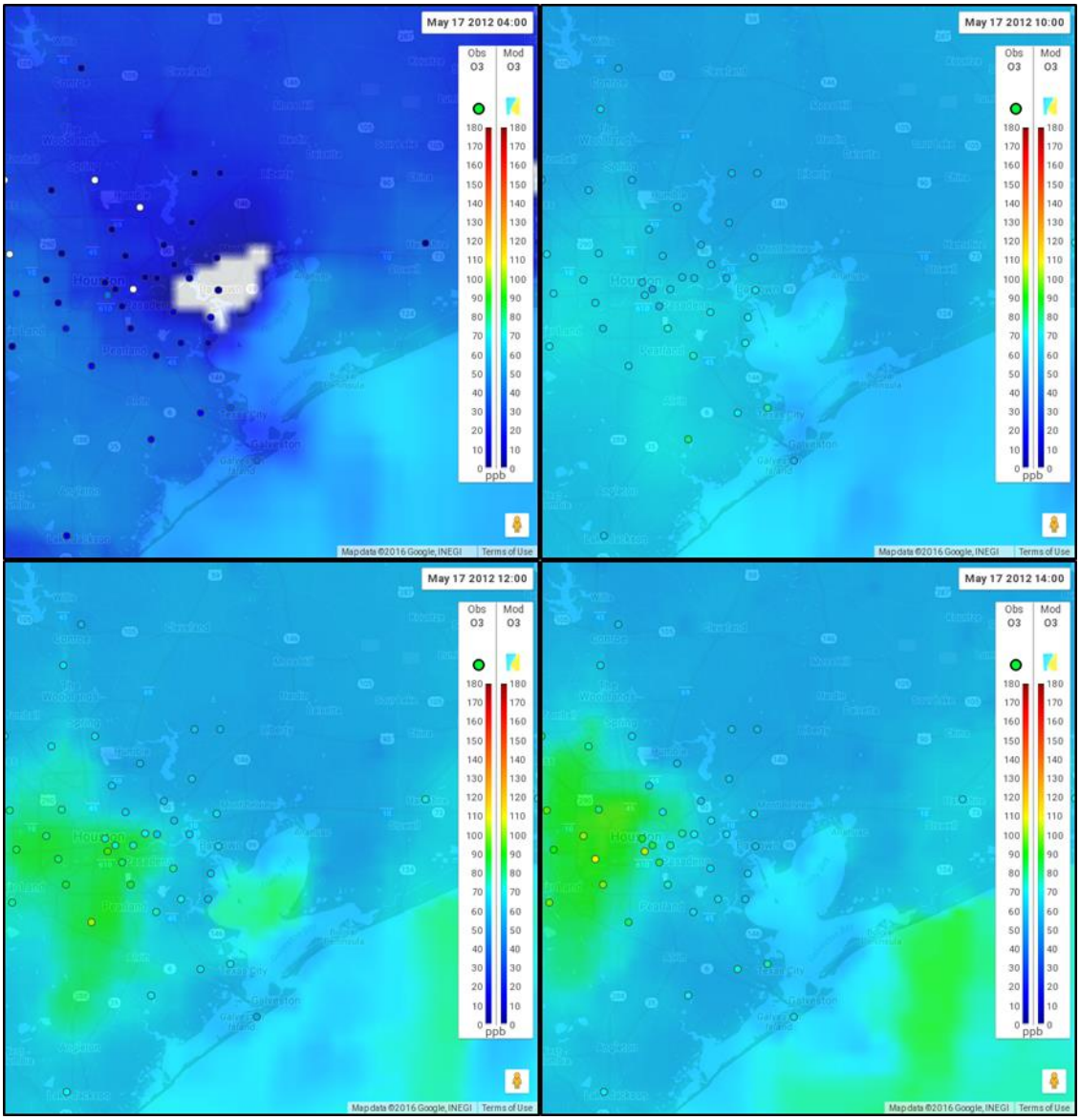

Figure 5-2: Modeled and Observed Ozone Concentrations on May 17, 2012

5.2 SEPTEMBER 19 THROUGH 21, 2012

September 19 through 21 was similar to the May period shown above. Figure 5-3: *Modeled and Observed Ozone Concentrations on September 19, 2012* shows very low observed and modeled ozone at 06:00 on September 19 (upper left panel). By 12:00 the model accurately places its highest ozone concentrations south and west of downtown Houston (upper right panel). The model captures well the slow southwest drift of the highest concentrations at 14:00 (lower left panel), but under-predicted the 85 ppb concentration at Manvel Croix Park - C84 by 21 ppb. The model peak is several kilometers southwest of Manvel Croix Park – C84 and was lower than observed peaks on that day, most likely due to modeled winds that were stronger and more organized than observed. Figure 5-4: *Section of Map Showing Observed and Modeled Wind Vectors at 14:00 on September 19, 2012* shows a portion of the wind map at 14:00 – modeled winds are shown in blue while observations are shown in red. The upper right panel of

the ozone concentration plot shows that by 18:00 the ozone plume was far to the southwest and very low ozone concentrations covered most of Houston.

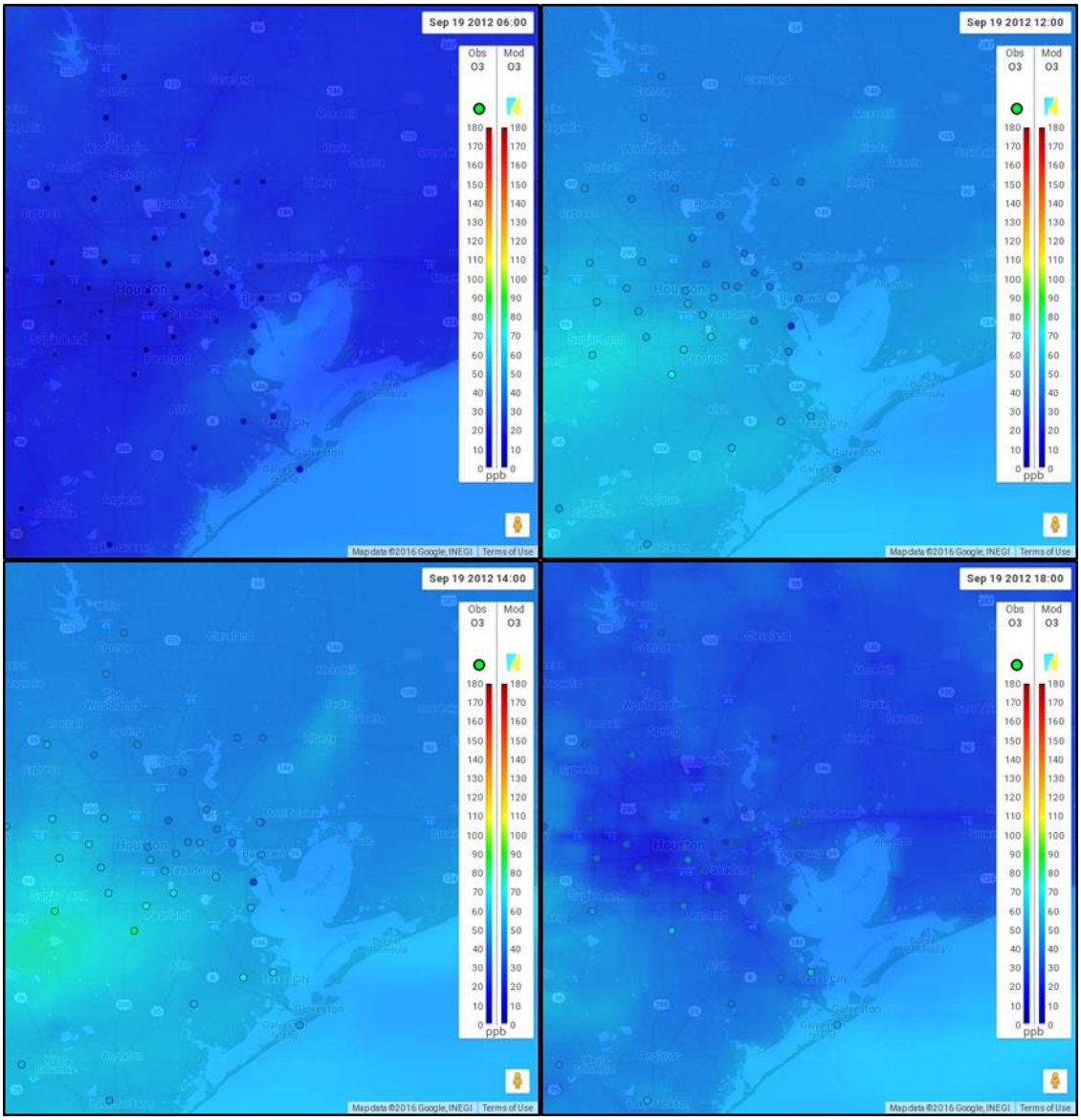

Figure 5-3: Modeled and Observed Ozone Concentrations on September 19, 2012

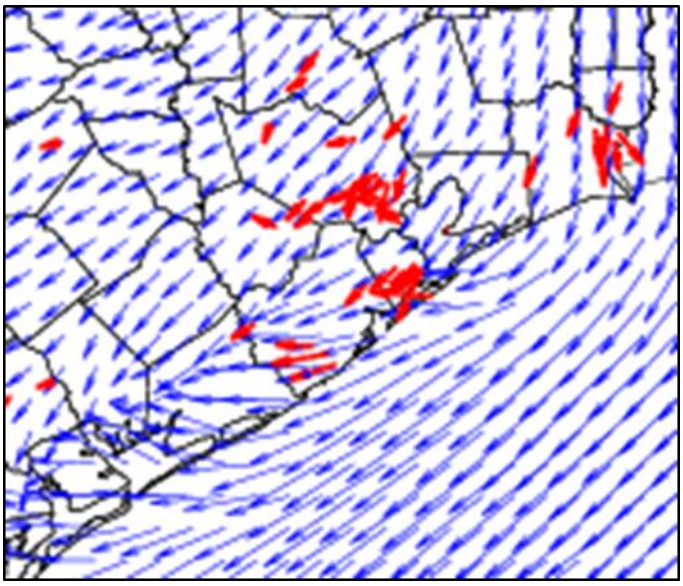

Figure 5-4: Section of Map Showing Observed and Modeled Wind Vectors at 14:00 on September 19, 2012

September 20 was similar to the previous day, except for a more westerly drift. Again too-strong modeled winds were responsible for pushing the ozone plume too far west and not allowing enough time to develop the peak one-hour concentration of 106 ppb observes at Manvel Croix Park – C84 on this day. Figure 5-5: *Modeled and Observed Ozone Concentrations on September 20, 2012* follows the same sequence as the previous figure: upper left 06:00, upper right 12:00, lower left 14:00, lower right 18:00.

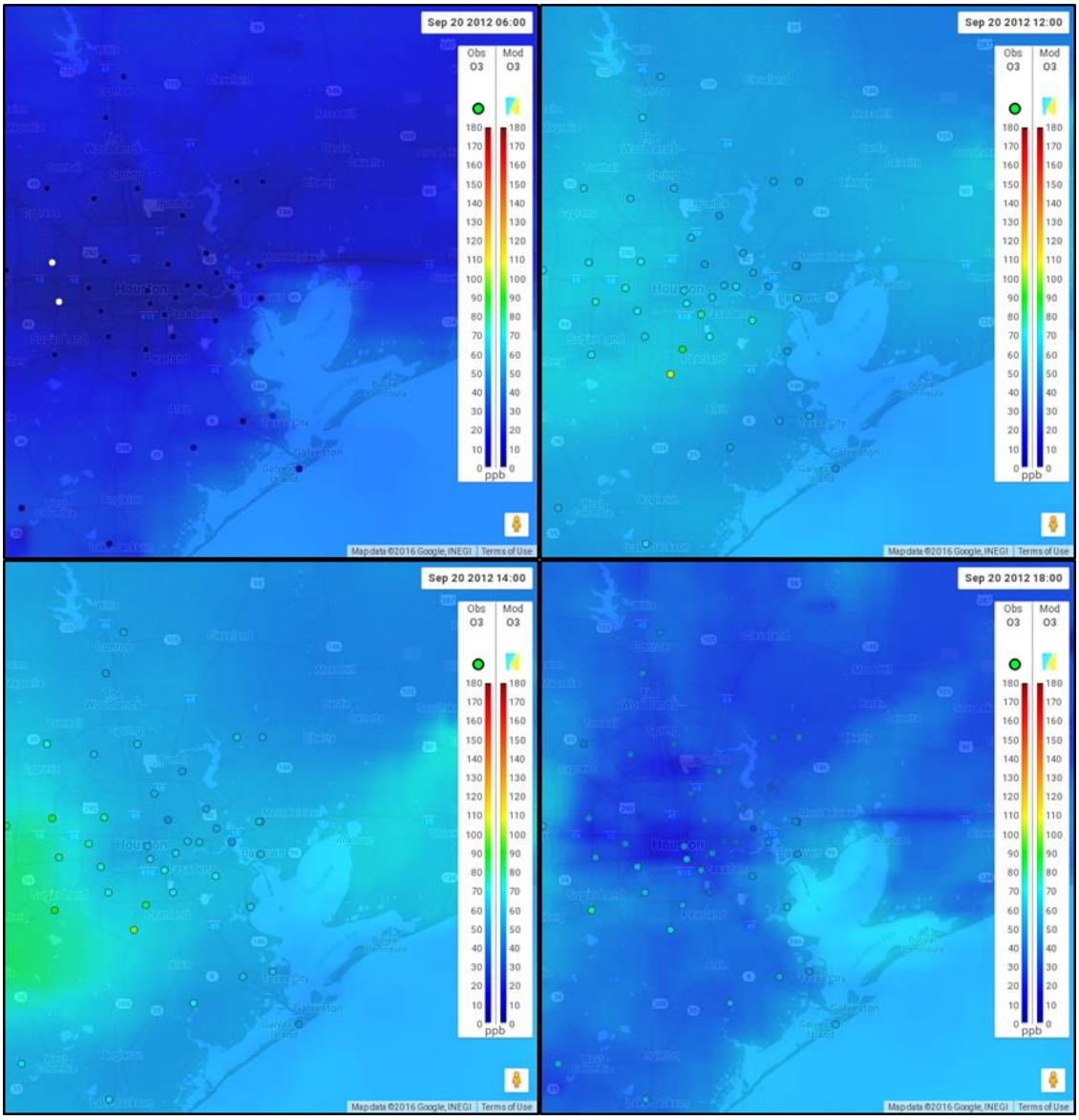

Figure 5-5: Modeled and Observed Ozone Concentrations on September 20, 2012

September 21 provided some relief for Manvel Croix Park by pushing the highest ozone almost due west (*Figure 5-6: Modeled and Observed Ozone Concentrations on September 21, 2012*). Similar to the two preceding days, the model does a very good job of moving the ozone plume in the correct direction. However, the model is unable to match the observed high concentrations at 14:00 seen at West Houston - C554 (106 ppb) or Lang - C408 (108 ppb) because of stronger and more organized winds than observed (Figure 5-7: *Section of Map Showing Observed and Modeled Wind Vectors at 14:00 on September 21, 2012*).

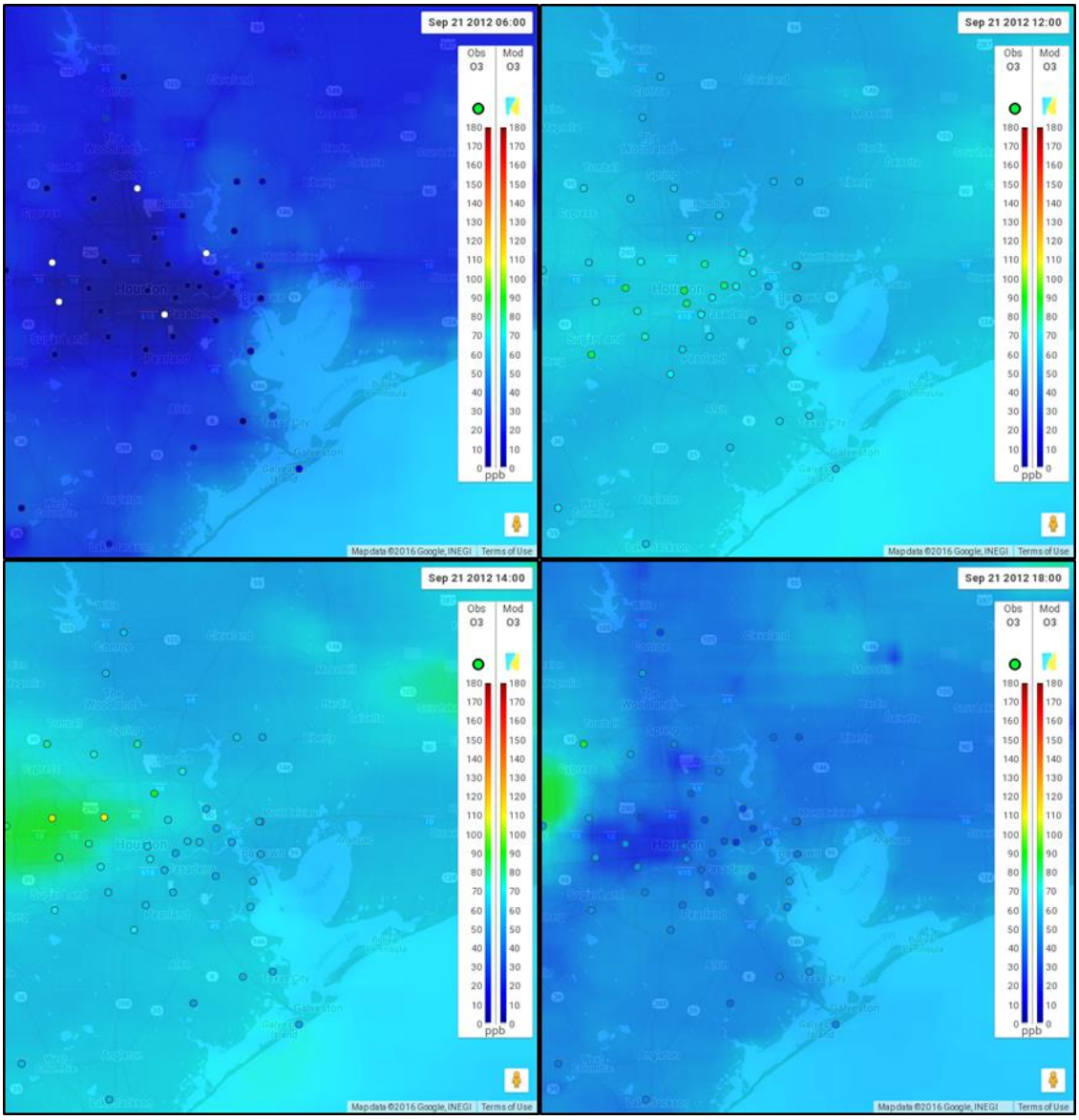

Figure 5-6: Modeled and Observed Ozone Concentrations on September 21, 2012

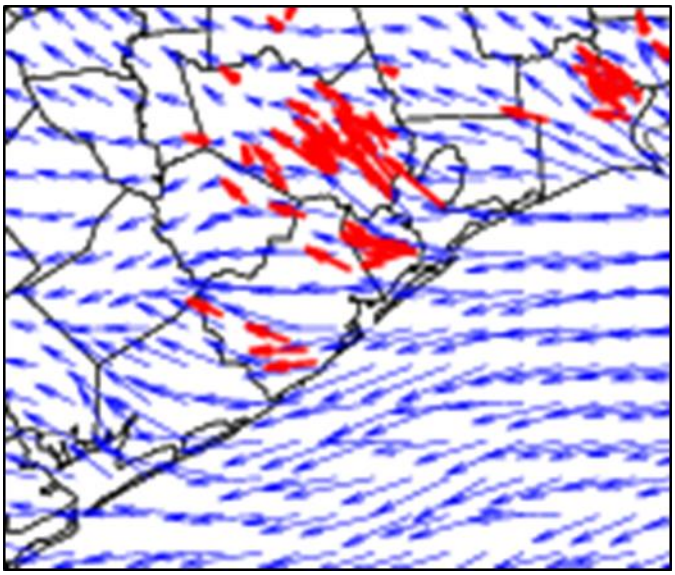

Figure 5-7: Section of Map Showing Observed and Modeled Wind Vectors at 14:00 on September 21, 2012

5.3 SUMMARY

Two selected episodic periods within the 2012 modeling platform illustrate the model's considerable skill in matching the time and placement of the observed ozone plumes. In the May period, the model matched the observations very well spatially, temporally, and in magnitude. In the September period the model also matched the observed ozone concentrations in time and direction, but higher-than-observed winds tended to push the highest concentrations farther from the city and also diminished the intensity of the ozone concentration peaks. Overall, however, the model is doing a very credible job of replicating ozone production in the region.

CHAPTER 6: ANTHROPOGENIC PRECURSOR CULPABILITY ANALYSIS

6.1 INTRODUCTION

Anthropogenic Culpability Precursor Analysis (APCA) is an optional probing tool in CAMx that can be used to apportion the modeled ozone concentration at a location in space and time among emission sources (including initial concentrations and influx through the domain borders). APCA can provide insight into understanding the causes of high ozone concentrations that occur in a region. The TCEQ ran APCA for both the 2012 baseline and 2017 future case; this section will focus primarily on the latter with limited comparison between the baseline and future case.

In the current application, the modeling domain was divided into three source regions: the eight HGB nonattainment counties (referred to as 'HGB'), the remainder of Texas (referred to as 'Texas – HGB'), and the remainder of the modeling domain ('Outside Texas'). These regions are shown in Figure 6-1: *APCA Source Regions*. Also shown are the four lateral boundaries, which are also considered source regions, along with (not shown) the top boundary of the three-dimensional grid.

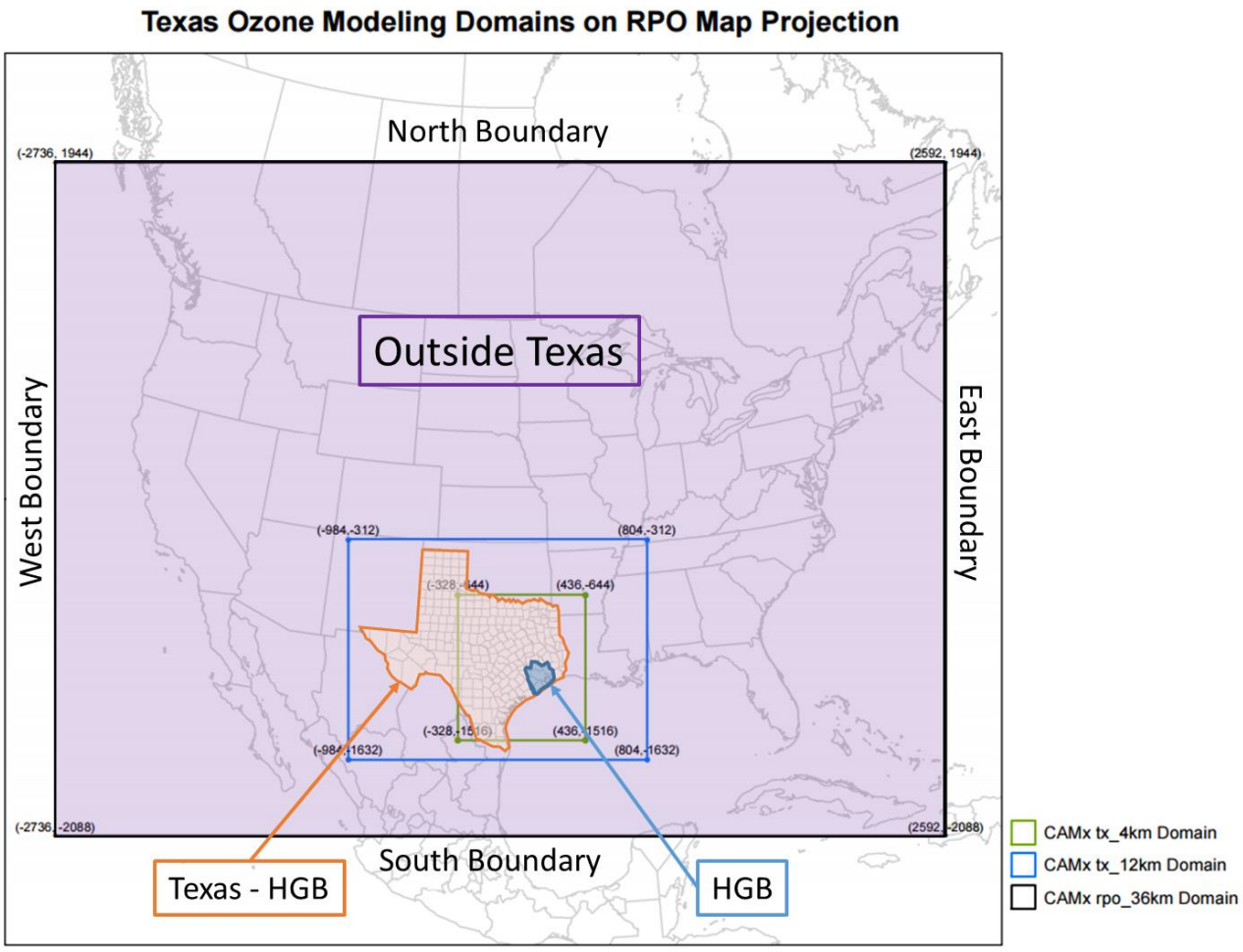

Figure 6-1: APCA Source Regions

Within source regions (excluding boundaries) certain emission source groups are defined to track contributions from various types of emitters. Table 6-1: *Aggregated Emission Source Categories* shows the emission groups defined for this analysis. In the analyses subsequently presented many of the individual groups are combined. Also, ozone produced from NO_X and VOC emissions are tracked separately by APCA but are generally combined for purposes of this discussion.

Table 6-1: Aggregated Emission Source Categories

Emission Category	Notes
On-Road Mobile	
Point Sources (EGU)	Does not include low-level sources associated with Electric Generation Units (EGUs)
Point Sources (non-EGU)	Includes all low-level point sources and all elevated point sources not identified as EGUs
Area Sources	
Biogenics	All source regions are combined in this discussion

Emission Category	Notes
Oil & Gas	Individual categories modeled for Haynesville, Barnett, and Eagle Ford Shale, Permian Basin activities, and Other; combined by region for this discussion
Non/Off-Road	Includes all non-road emissions plus off-road sources except certain ships (see below)
Ships	All ocean-going vessels, plus harbor vessels in the HGB and Beaumont-Port Arthur areas. Other areas' harbor vessels are included in Non/Off Road.
Initial Conditions	Inherited from global model (GEOS-Chem which provided initial concentration data to start the model runs
Boundary Conditions	Concentration data along four "walls" (W,N,E,S) of 36-km domain, plus the "ceiling", also inherited from GEOS-Chem.

6.2 MANVEL CROIX PARK (C84)

The Manvel Croix Park (C84) monitor is of particular interest because it measured the highest design value in the HGB region from 2009 through 2015. This section discusses the sources that contribute to eight-hour ozone at this location. Additional monitors will be discussed in subsequent sections but not as extensively. Concentration plots in this chapter show running eight-hour ozone totals and source contributions, and hour (x-axis) represents the start of each 8-hour period. For example, ozone contribution plotted for hour 10 represents the average of hourly concentrations between hours 10 and 17, inclusive. The term MDA8 applies specifically to the highest eight-hour average modeled in a 24-hour period.

Manvel Croix Park (C84) is located in northern Brazoria County, as shown previously in Figure 3-30. Figure 6-2: *Baseline (top) and Future (bottom) Modeled Contributions to June Eight-Hour Ozone at Manvel Croix Park (C84)* shows baseline contribution by region to 8-hour average ozone concentrations at Manvel Croix Park (C84) for June 2012, together with the 2017 projected contributions, averaged over the 3x3 grid cell array with the monitor located in the central cell. The differences between the 2012 baseline and 2017 future case are fairly subtle but evident. For example on June 26, the MDA8 concentration dropped from 93.99 ppb to 88.19 ppb. This decrease will be discussed later.

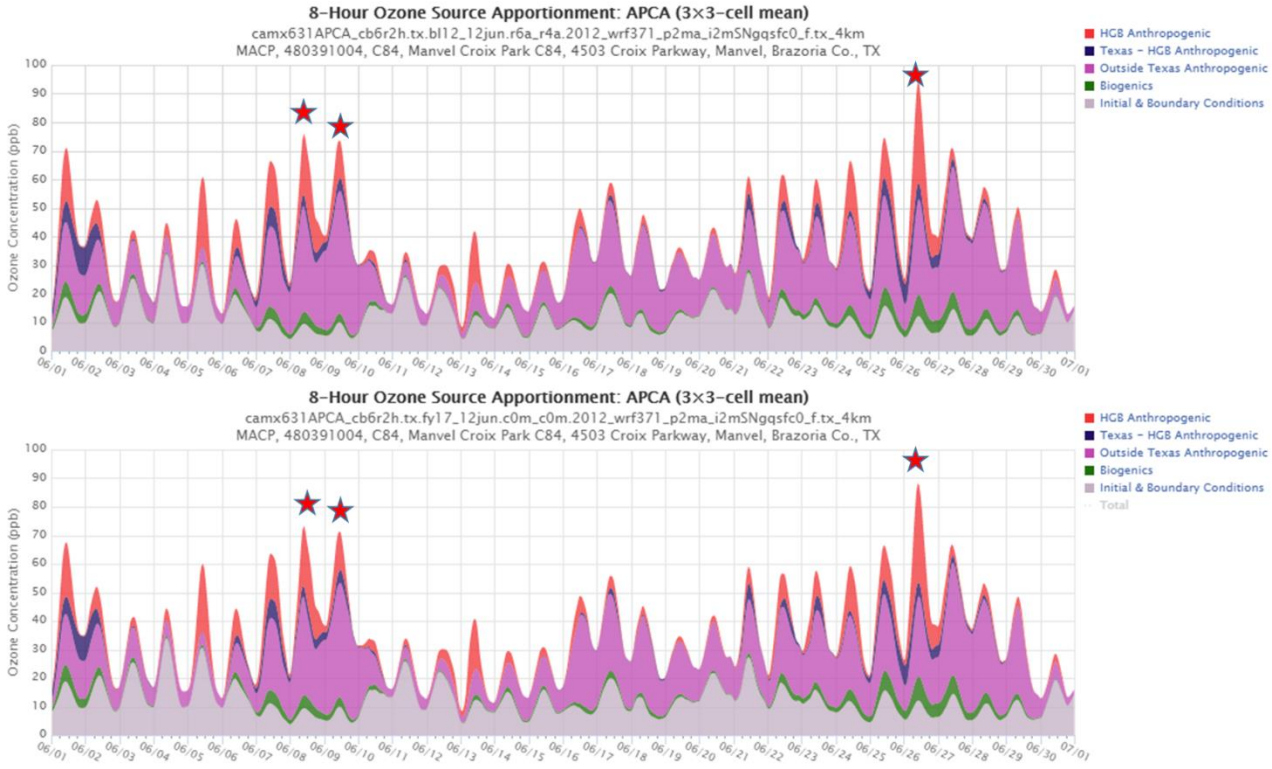

Figure 6-2: Baseline (top) and Future (bottom) Modeled Contributions to June Eight-Hour Ozone at Manvel Croix Park (C84)

An interesting feature of the plots for both years is the minor contribution from sources in Texas outside the HGB area, together with the dominance of contribution from outside Texas on most days. The local contribution varies but is, not unexpectedly, highest on the days with the highest modeled MDA8 concentration. Biogenic contributions are relatively small but are at their highest on June 26, the day with the highest MDA8 concentration of the entire five-month modeling period. The contribution from initial and boundary conditions varies considerably but is notably quite small on some of the highest ozone days. Days marked with a red star are among the ten days used in the top ten day future design value calculation recommended in the EPA's December 2014 *Draft Modeling Guidance for Demonstrating Attainment of Air Quality Goals for Ozone, PM2.5, and Regional Haze.*

Figure 6-2 does not distinguish between contributions from NO_X and those from VOC. While anthropogenic VOC emissions, especially highly-reactive VOCs, can contribute to ozone formation and in some cases can cause short term ozone "spikes" with very high concentrations over a few hours, APCA modeling shows a very limited role for VOC at Manvel Croix Park (C84). Figure 6-3: *June Modeled Future Anthropogenic Eight-Hour Ozone at Manvel Croix Park (C84); Local and Regional NO_X and VOC Attribution* divides anthropogenic 8-hour ozone at Manvel Croix Park (C84) between locally-generated and regional (i.e. outside HGB) ozone, and further segregates these into VOC-attributed and NO_X-attributed ozone (biogenic and initial and boundary condition-attributed ozone is omitted from the figure). On the days in June used in the DV_F calculation, total eight-hour ozone attributed to VOC by APCA is less than 3 ppb at the peak hours, although locally-emitted VOC does generate over 5 ppb of MDA8 ozone on some lower-ozone days.

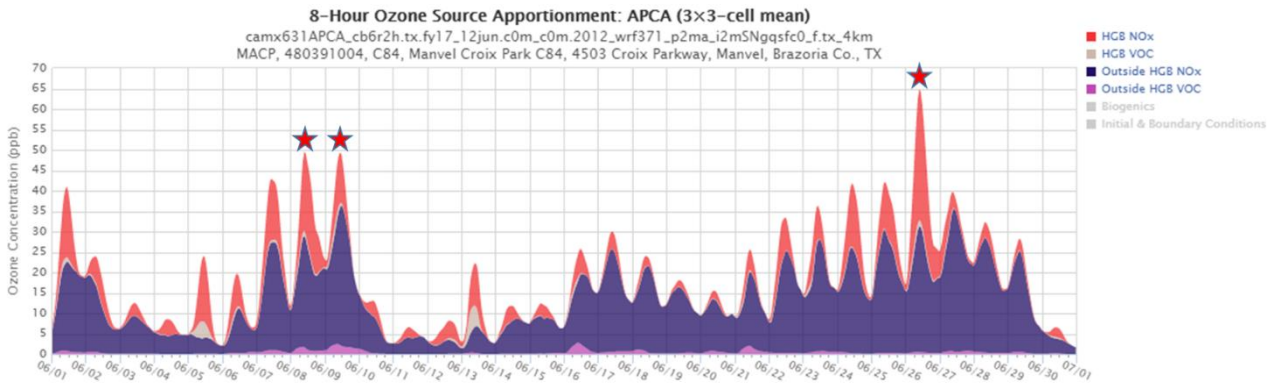

Figure 6-3: June Modeled Future Anthropogenic Eight-Hour Ozone at Manvel Croix Park (C84); Local and Regional NO_x and VOC Attribution

Table 6-2: *June 26 Baseline and Future Contributions to Manvel Croix Park (C84) MDA8 Ozone by Source Region* breaks down the contributions on June 26 to MDA8 ozone for the baseline and future cases. Contributions from all three geographic regions decreased, with the largest decrease of over 5 ppb coming from sources outside Texas. The contribution from Texas – HGB decreased by nearly 1 ppb, while the ozone contribution from the HGB region itself decreased by 0.7 ppb, despite significant population and economic growth. These reductions were countered somewhat by combined increases from initial and boundary conditions and biogenics of about 1 ppb. While the boundary concentrations increased between 2012 and 2017, biogenic emissions remained constant; the increase to this source likely resulted from the model attributing more ozone production to biogenic VOC and NO_x in regions where anthropogenic NO_x concentrations were reduced.

Table 6-2: June 26 Baseline and Future Contributions to Manvel Croix Park (C84) MDA8 Ozone by Source Region

Source Region	Baseline Contribution (ppb, *percent*)	Future Case Contribution (ppb, *percent*)
HGB	35.64 ppb, *37.91%*	34.94 ppb, *39.62%*
Texas - HGB	6.19 ppb, *6.59%*	5.24 ppb, *5.94%*
Outside Texas	32.73 ppb, *34.83%*	27.7 ppb, *31.4%*
Biogenics	7.44 ppb, *7.92%*	8.24 ppb, *9.35%*
Initial and Boundary Conditions	11.99 ppb, *12.75%*	12.07 ppb, *13.69%*
Total	93.99 ppb, *100%*	88.19 ppb, *100%*

Figure 6-4: *May, August and September Modeled Future Eight-Hour Ozone Contributions by Source Region at Manvel Croix Park (C84)* shows modeled 2017 source contributions for Manvel Croix Park (C84) for the months of May (top), August (middle), and September (bottom). July is not shown because MDA8 ozone did not exceed 50 ppb at this location during the entire month. Again, days marked with a red star are among the ten used for calculating the future design value for this monitor.

As was the case with the June days used for the DV_F calculation, all the starred days in May, August, and September have a substantial local contribution ranging from about

15 to nearly 40 ppb. With the exception of August 20, the selected days are characterized by relatively low contributions from initial and boundary conditions (less than 16 ppb), biogenics, and Texas – HGB. August 20 is unusual in several ways. First, the nine-cell average depicted in the figure is slightly lower than that on August 21, even though the latter was not used in the DV_F calculation. This occurs because the DV_F calculation uses the maximum of nine grid cells rather than the average (since August 21 had the eleventh highest nine-cell maximum it was not used in the DV_F calculation). Second, August 20 has a relatively high contribution from biogenics (almost 8 ppb) and a small contribution from outside Texas (less than 10 ppb). The contribution from Texas – HGB was the largest contributor at over 19 ppb, higher than the local share at just above 15 ppb.

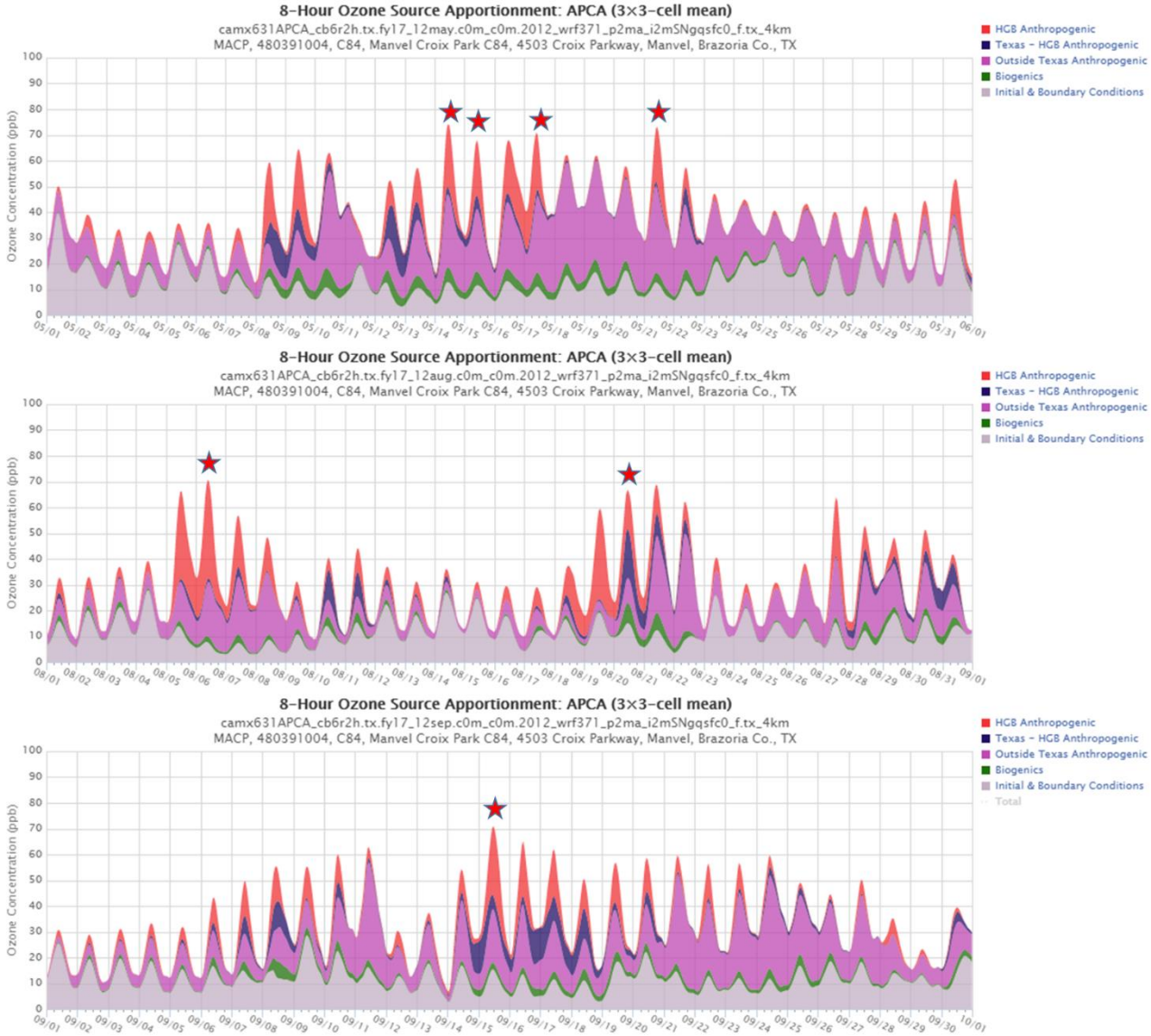

Figure 6-4: May, August and September Modeled Future Eight-Hour Ozone Contributions by Source Region at Manvel Croix Park (C84)

To see which source types are contributing the most to ozone formation, each of the source groups was further divided by source category as shown in the following figures (biogenics are included in the figures showing initial and boundary conditions). Figure 6-5: *June Initial and Boundary Conditions and Biogenics Modeled Future Eight-Hour Ozone Contributions at Manvel Croix Park (C84)* shows 2017 modeled contributions from each of the four lateral and the top boundary, initial conditions, and biogenics at Manvel Croix Park (C84) for June. The top chart shows the contributions along with the modeled totals depicted by the dotted line, while the bottom figure scales the chart to the subject data allowing closer examination. Initial conditions are essentially nonexistent (due to the long spin-up period used) and top boundary conditions are equally negligible. As expected, South boundary conditions dominate on low-ozone days, while South, West, and North boundary conditions each contribute roughly comparable amounts on the three days included in the future design value calculation.

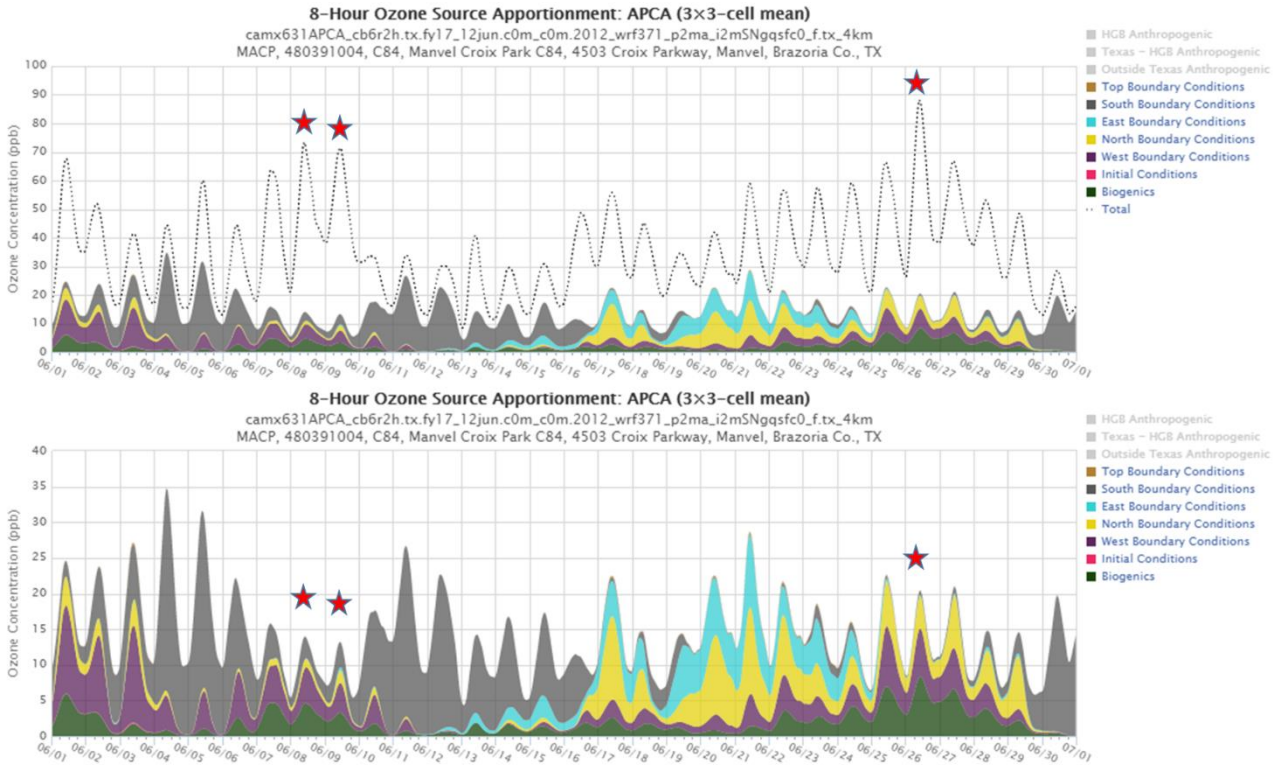

Figure 6-5: June Initial and Boundary Conditions and Biogenics Modeled Future Eight-Hour Ozone Contributions at Manvel Croix Park (C84)

Figure 6-6: *June Outside Texas Modeled Future Eight-Hour Ozone Contributions by Source Category at Manvel Croix Park (C84)* presents a similar breakdown of June eight-hour ozone contributors by source categories for the sources outside Texas. Area sources and non-EGU point sources are the primary contributors to MDA8 ozone on June 8 and 9, with sizable contributions from both on-road and non/off-road mobile sources but little from oil & gas. On the June 9, electric generation and ships also make substantive contributions to MDA8 ozone. On June 26, area sources from outside Texas make only a minor contribution and ship contributions are negligible. Oil and gas makes a small contribution of around 2.5 ppb, and on- and non/off-road mobile

each contribute upwards of 6 ppb. Electric generation contributes about 5.5 ppb followed by non-EGU point sources at about 4 ppb.

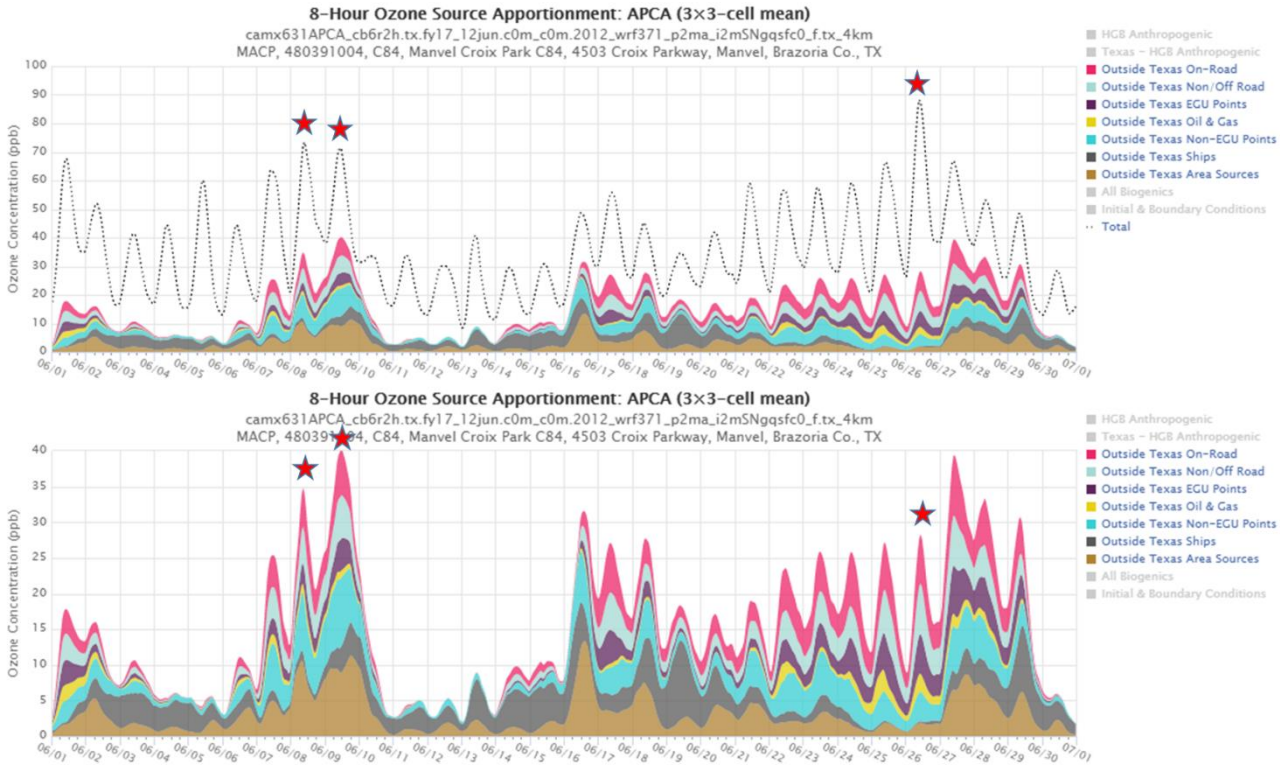

Figure 6-6: June Outside Texas Modeled Future Eight-Hour Ozone Contributions by Source Category at Manvel Croix Park (C84)

Figure 6-7: *June Texas – HGB Modeled Future Eight-Hour Ozone Contributions by Source Category at Manvel Croix Park (C84)* breaks down the non-HGB Texas contribution to eight-hour ozone at Manvel Croix Park (C84) for June. These sources contribute less than 10 ppb throughout the entire month of August. On June 8 and 9 Texas non-EGU point sources contribute 2 to 3 ppb to MDA8 ozone. On-road mobile contributes a little more than 1 ppb, with the remaining sources contributing less than 1 ppb. On June 26 the largest contributor to MDA8 ozone is on-road mobile at 2.3 ppb followed by non-EGU points at just over 1 ppb. Oil and gas and non/off-road both contribute just over 0.75 ppb.

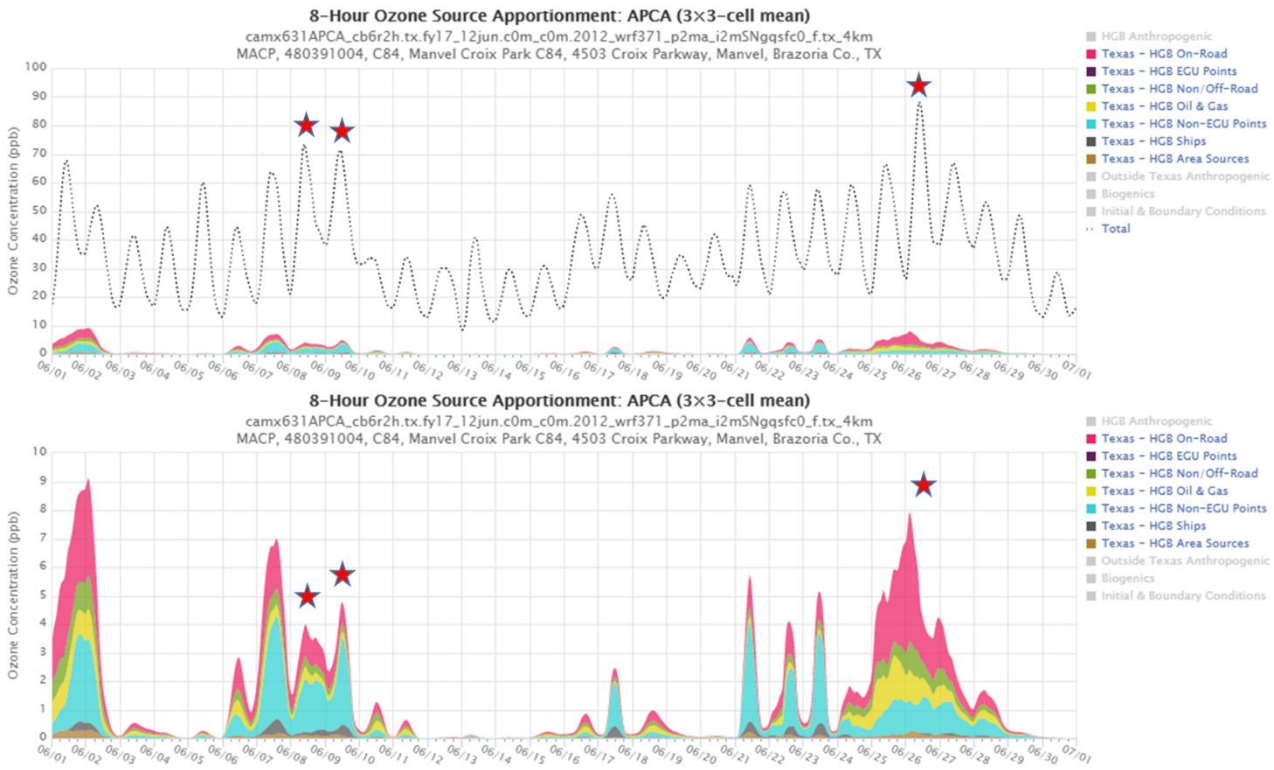

Figure 6-7: June Texas – HGB Modeled Future Eight-Hour Ozone Contributions by Source Category at Manvel Croix Park (C84)

It is worth examining the non-HGB Texas contribution for August, since on August 20 this source made a substantial contribution to MDA8 ozone, as noted earlier. On this day on-road (9.6 ppb), non/off-road (3.9 ppb), oil and gas (2.6 ppb), and non-EGU point sources (2.0 ppb) combined to provide almost all of the contribution from Texas – HGB (~20 ppb), as shown in Figure 6-8: *August Texas – HGB Modeled Future Eight-Hour Ozone Contributions by Source Category at Manvel Croix* Park (C84).

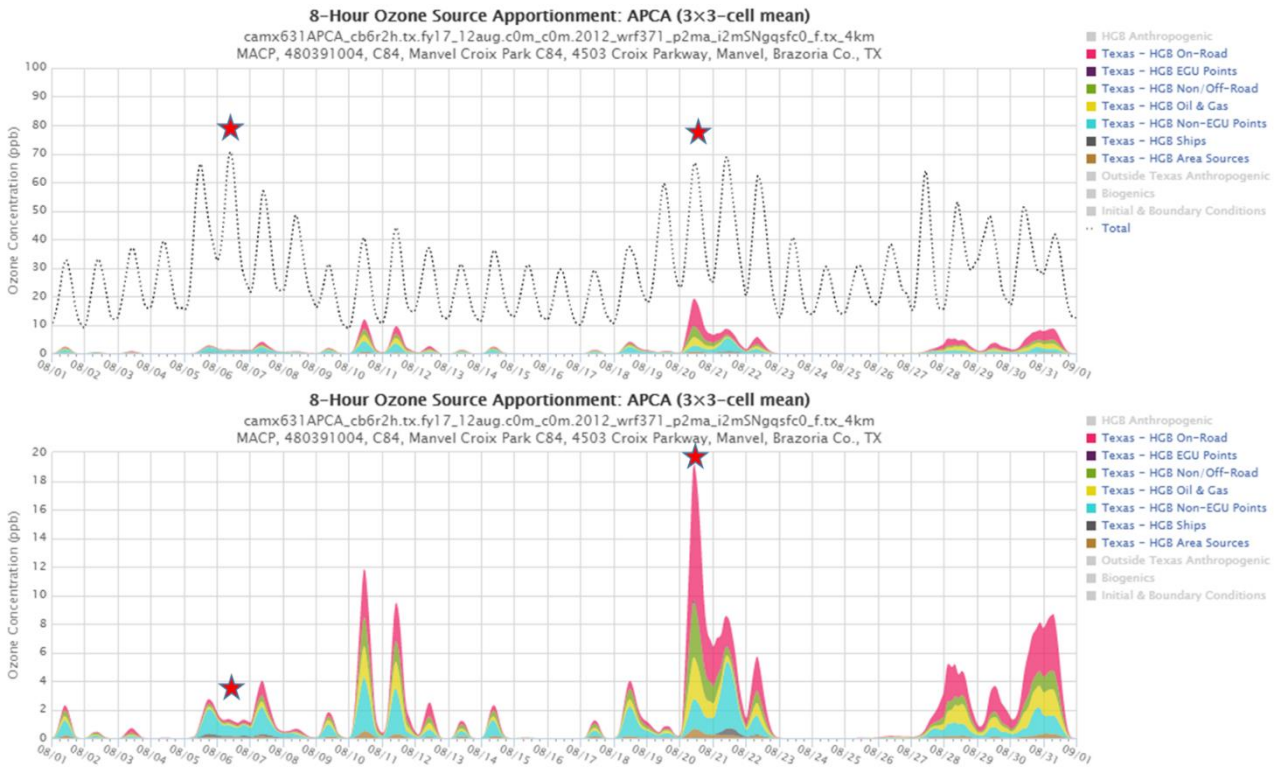

Figure 6-8: August Texas – HGB Modeled Future Eight-Hour Ozone Contributions by Source Category at Manvel Croix Park (C84)

Figure 6-9: *June HGB Modeled Future Eight-Hour Ozone Contributions by Source Category at Manvel Croix Park (C84)* shows the makeup of the HGB contribution to eight-hour ozone at Manvel C84 for June. For each day in June, on-road mobile, non/off-road mobile, and non-EGU point sources constitute the bulk of the ozone contributions, with some assistance from area sources on a few high days. HGB electricity generation contributes less than 1.5 ppb on any day, and oil and gas and ships only contribute marginally.

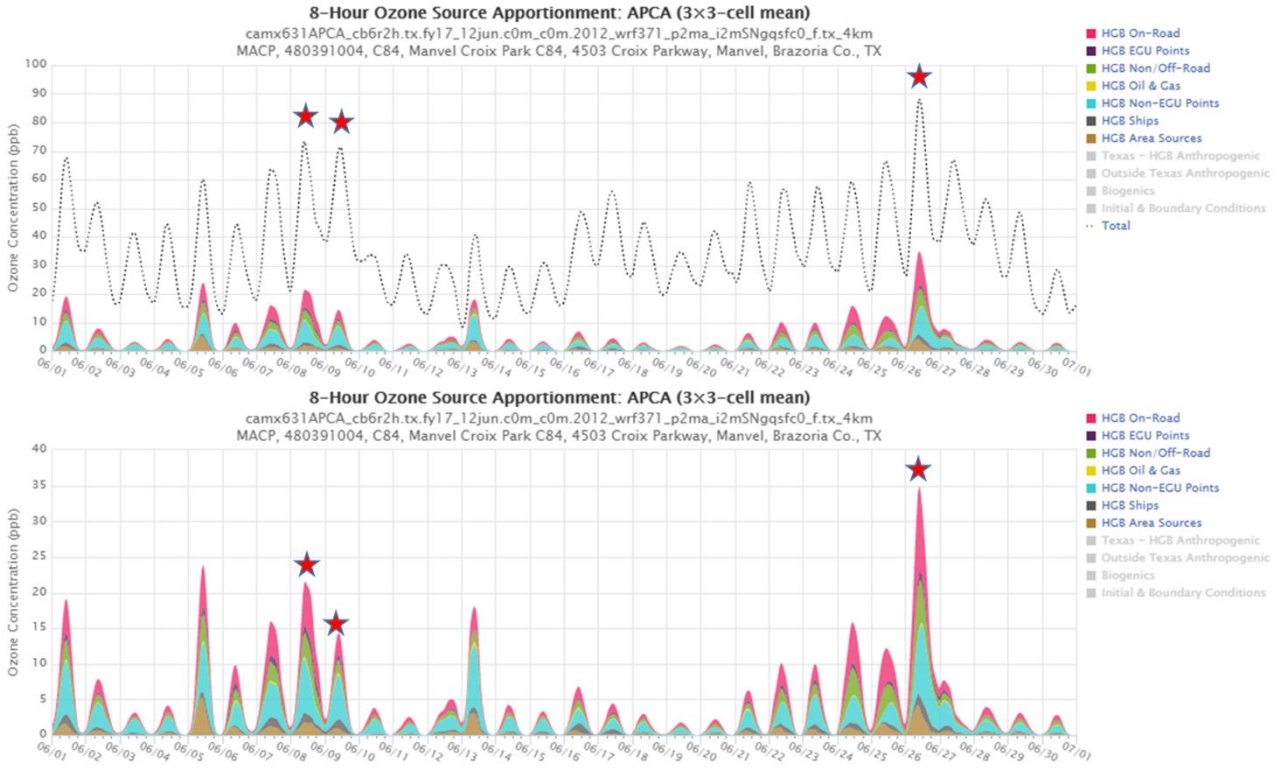

Figure 6-9: June HGB Modeled Future Eight-Hour Ozone Contributions by Source Category at Manvel Croix Park (C84)

Table 6-3: *Contributions from HGB Source Categories to Modeled Future 8-Hour Ozone for Three Selected Days at Manvel Croix Park (C84)* shows contributions from the various emission categories for each of the three June days used in the DV_F calculation. Contributions are shown in ppb, as a percent of the HGB contribution, and as a percent of each day's MDA8 concentration. On the selected days with a large local contribution, on-road mobile (22 to 35%) and non-EGU point sources (27 to 42%) are the main contributors.

Table 6-3: Contributions from HGB Source Categories to Modeled Future 8-Hour Ozone for Three Selected Days at Manvel Croix Park (C84)

Category	**June 8 ppb**, *% of HGB*, % of MDA8	**June 9 ppb**, *% of HGB*, % of MDA8	**June 26 ppb**, *% of HGB*, % of MDA8
HGB On-Road	**6.01 ppb** *28.07%* 8.19%	**3.09 ppb** *21.99%* 4.33%	**12.12 ppb** *34.68%* 13.74%
HGB EGU Points	**1.06 ppb** *4.94%* 1.44%	**0.76 ppb** *5.37%* 1.06%	**1.27 ppb** *3.63%* 1.44%
HGB Non/Off-Road	**3.27 ppb** *15.29%* 4.46%	**1.83 ppb** *13.02%* 2.56%	**6.62 ppb** *18.94%* 7.51%

Category	June 8 ppb, *% of HGB*, % of MDA8	June 9 ppb, *% of HGB*, % of MDA8	June 26 ppb, *% of HGB*, % of MDA8
HGB Oil & Gas	**0.26 ppb** *1.24%* 0.36%	**0.29 ppb** *2.07%* 0.41%	**0.28 ppb** *0.79%* 0.31%
HGB Non-EGU Points	**7.66 ppb** *35.77%* 10.44%	**5.91 ppb** *42.01%* 8.27%	**8.98 ppb** *25.69%* 10.18%
HGB Ships	**1.33 ppb** *6.21%* 1.81%	**1.37 ppb** *9.78%* 1.92%	**1.67 ppb** *4.79%* 1.90%
HGB Area Sources	**1.82 ppb** *8.48%* 2.47%	**0.81 ppb** *5.75%* 1.13%	**4.01 ppb** *11.48%* 4.55%
HGB Total Contribution	**21.41 ppb** *100%* 29.18%	**12.67 ppb** *100%* 19.68%	**34.95 ppb** *100%* 39.64%
MDA8	**73.39 ppb**	**71.43 ppb**	**88.19 ppb**

Finally, source apportionment was used to disaggregate the 2017 DV_F for Manvel Croix Park (C84). The APCA results presented so far have been based on the raw 2017 model predictions, but the DV_F used for attainment modeling uses the modeling in a relative sense. Briefly, for each regulatory monitor the ten modeled days having the highest baseline MDA8 ozone concentration near the monitor are selected for calculating the relative response factor (RRF). These highest baseline MDA8 values are averaged across the ten selected days. The same process is applied to the future case modeling except the same ten days are used, and the ratio of the future average MDA8 concentration to the baseline average is the monitor's RRF. The RRF is multiplied by the monitor's observed three-year average baseline design value (DV_B) to find the monitor's DV_F.

To disaggregate the DV_F for a monitor, the APCA-estimated component concentrations were averaged across the ten selected days and the monitor's DV_F was apportioned into components accordingly. The DV_F components are shown in Table 6-4: *Modeled 2017 DV_F Components for Manvel Croix Park (C84) (ppb)*. These results are also displayed graphically in Figure 6-10: *Modeled 2017 DV_F Components for Manvel Croix Park (C84)*. The contribution from HGB sources is slightly less than the contribution from sources outside Texas but within the modeling domain (i.e. not counting boundary conditions, which add another 12.4 ppb).

Table 6-4: Modeled 2017 DV_F Components for Manvel Croix Park (C84) (ppb)

Category	IC/BC	Biogenics	HGB	Texas - HGB	Outside Texas	Source Category Total
On-Road			9.70	1.15	5.81	**16.66**
EGU Points			1.10	0.96	3.75	**5.81**
Non/Off Road			5.42	0.83	5.18	**11.43**

Category	IC/BC	Biogenics	HGB	Texas - HGB	Outside Texas	Source Category Total
Oil & Gas			0.23	0.79	1.48	**2.50**
Non-EGU Points			6.70	1.34	5.56	**13.60**
Ships			1.22	0.08	1.67	**2.97**
Area Sources			3.82	0.20	4.79	**8.81**
Source Region Total	**12.38**	**5.23**	**28.19**	**5.35**	**28.24**	**79.39**

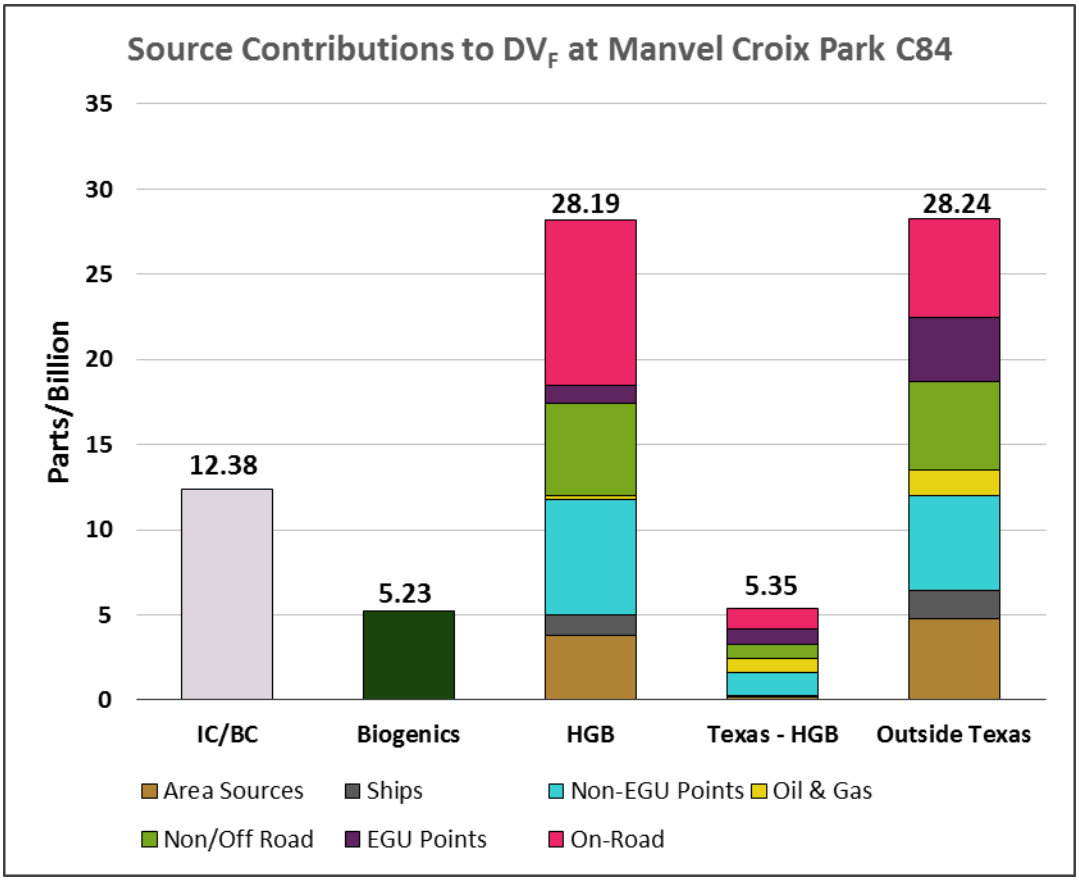

Figure 6-10: Modeled 2017 DV_F Components for Manvel Croix Park (C84)

6.3 ALDINE (C8)

Figure 6-11: *May through September Modeled Future Eight-Hour Ozone Contributions by Source Region at Aldine (C8)* shows modeled future contributions by region for all five months (in chronological order from top to bottom) modeled for the Aldine (C8) monitor (refer to Figure 3-14 for location), with days used in the DV_F calculation noted by red stars. The selected days early in the season tended to be dominated by emissions from outside Texas, but as the season progressed local sources became more dominant with several days having 50% or more local contribution to MDA8 ozone. Texas sources outside HGB played only a minor part on any of the top ten days at this location.

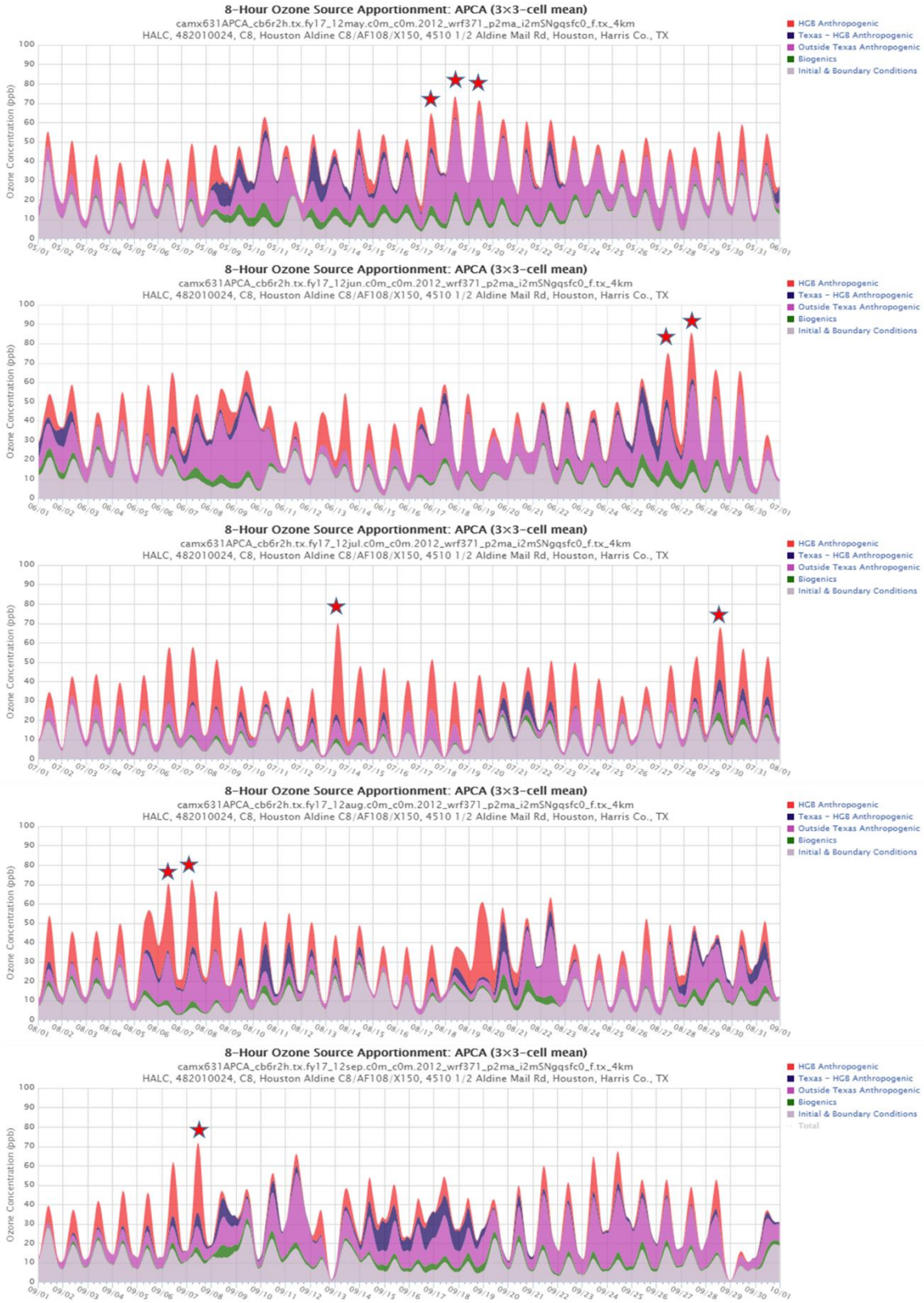

Figure 6-11: May through September Modeled Future Eight-Hour Ozone Contributions by Source Region at Aldine (C8)

Table 6-5: *Contributions from HGB Source Categories to Modeled Future 8-Hour Ozone for Three Selected Days at Aldine (C8)* examines the local contributions to future modeled MDA8 ozone for the three selected days having the largest fraction of local emissions: July 13, August 6, and September 7. On-road mobile sources contribute the largest share of locally-produced ozone, between 30 and 42%, with non/off-road sources contributing between 18 and 23%. HGB non-EGU point sources contribute from 10 to 24%.

Table 6-5: Contributions from HGB Source Categories to Modeled Future 8-Hour Ozone for Three Selected Days at Aldine (C8)

Category	**July 13 ppb**, *% of HGB*, % of MDA8	**August 7 ppb**, *% of HGB*, % of MDA8	**September 7 ppb**, *% of HGB*, % of MDA8
HGB On-Road	**14.49 ppb** *30.0%* 20.6%	**10.80 ppb** *30.63%* 15.25%	**15.02 ppb** *41.17%* 20.93%
HGB EGU Points	**1.79 ppb** *3.71%* 2.55%	**1.8 ppb** *5.09%* 2.54%	**2.08 ppb** *5.71%* 2.90%
HGB Non/Off-Road	**8.61 ppb** *17.82%* 12.24%	**8.21 ppb** *23.28%* 11.59%	**8.40 ppb** *23.03%* 11.71%
HGB Oil & Gas	**0.68 ppb** *1.41%* 0.97%	**0.36 ppb** *1.03%* 0.51%	**0.21 ppb** *0.58%* 0.29%
HGB Non-EGU Points	**9.2 ppb** *19.04%* 13.08%	**8.75 ppb** *24.81%* 12.35%	**3.67 ppb** *10.07%* 5.12%
HGB Ships	**0.88 ppb** *1.83%* 1.26%	**1.52 ppb** *4.31%* 2.15%	**0.73 ppb** *2.01%* 1.02%
HGB Area Sources	**12.65 ppb** *26.2%* 17.99%	**3.83 ppb** *10.85%* 5.40%	**6.36 ppb** *17.44%* 8.87%
HGB Total Contribution	**48.31 ppb** *100%* 68.68%	**35.27 ppb** *100%* 49.79%	**36.48 ppb** *100%* 50.48%
MDA8	**70.34 ppb**	**70.84 ppb**	**71.75 ppb**

Finally, the breakdown of contributions to the DV_F at Aldine (C8) is shown in Table 6-6: *Modeled 2017 DV_F Components for Aldine (C8) (ppb)* and Figure 6-12: *Modeled Future DV_F Components for Aldine (C8).* At this site, HGB sources contribute about 3 ppb more ozone to the DV_F than out-of-state sources (not counting boundary conditions).

Table 6-6: Modeled 2017 DV_F Components for Aldine (C8) (ppb)

Category	IC/BC	Biogenics	HGB	Texas - HGB	Outside Texas	Source Category Total
On-Road			8.56	0.57	4.80	**13.93**
EGU Points			1.46	0.52	3.39	**5.37**
Non/Off Road			5.64	0.44	4.28	**10.36**
Oil & Gas			0.24	0.53	1.36	**2.13**
Non-EGU Points			6.76	1.02	4.46	**12.24**
Ships			1.31	0.05	2.51	**3.87**
Area Sources			3.90	0.11	3.89	**7.90**
Source Region Total	**12.17**	**4.64**	**27.87**	**3.24**	**24.69**	**72.61**

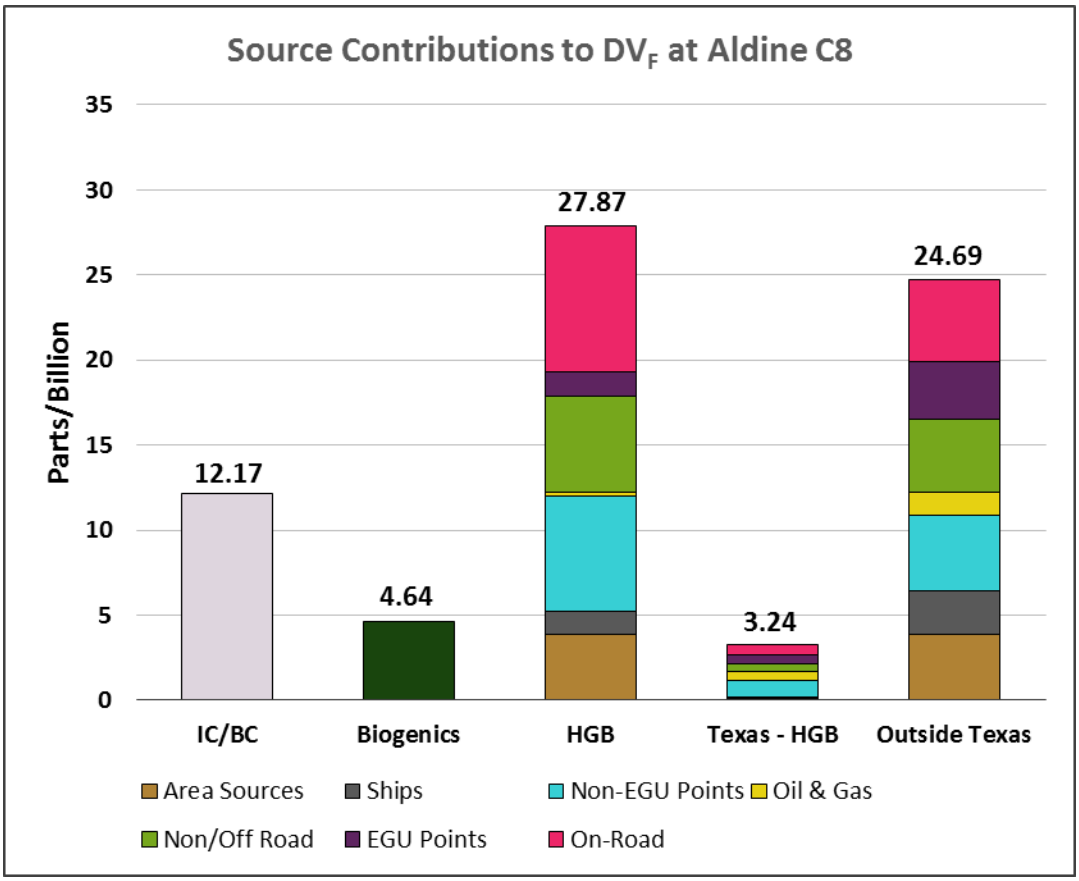

Figure 6-12: Modeled 2017 DV_F Components for Aldine (C8)

6.4 DEER PARK (C35)

Deer Park (C35) is located south of the main Ship Channel industrial area (refer to Figure 3-20). In the past decade Deer Park (C35) had design values that contended for the area-wide maximum; as recently as 2012 its design value of 84 ppb was the highest

in Harris County (area-wide maximum was 88 ppb), but since then it has seen design values well below the maximum.

The ten days selected for calculating the DV_F for Deer Park (C35) were all in May, June, and August as shown in Figure 6-13: *May, June, and August Modeled Future Eight-Hour Ozone Contributions by Source Region at Deer Park (C35)*. May 19 and 20 were dominated by out-of-state ozone with little local contribution, but the May 21 saw a sizable local contribution. The largest contributor on both June 7 and 9 was also from outside Texas, but both local and other Texas sources made significant contributions. The consecutive days of June 26 and 27 showed a remarkable contrast, with the former having a local contribution nearly as large as that from outside Texas (26.1 ppb vs. 29.7 ppb), but having a relatively small local contribution (7.2 ppb) on the latter, which was dominated by contributions from out-of-state (41.0 ppb). The situation is similar for August 20 and 21, except for a relatively large contribution from Texas outside HGB on both days. August 6, on the other hand, was primarily locally driven.

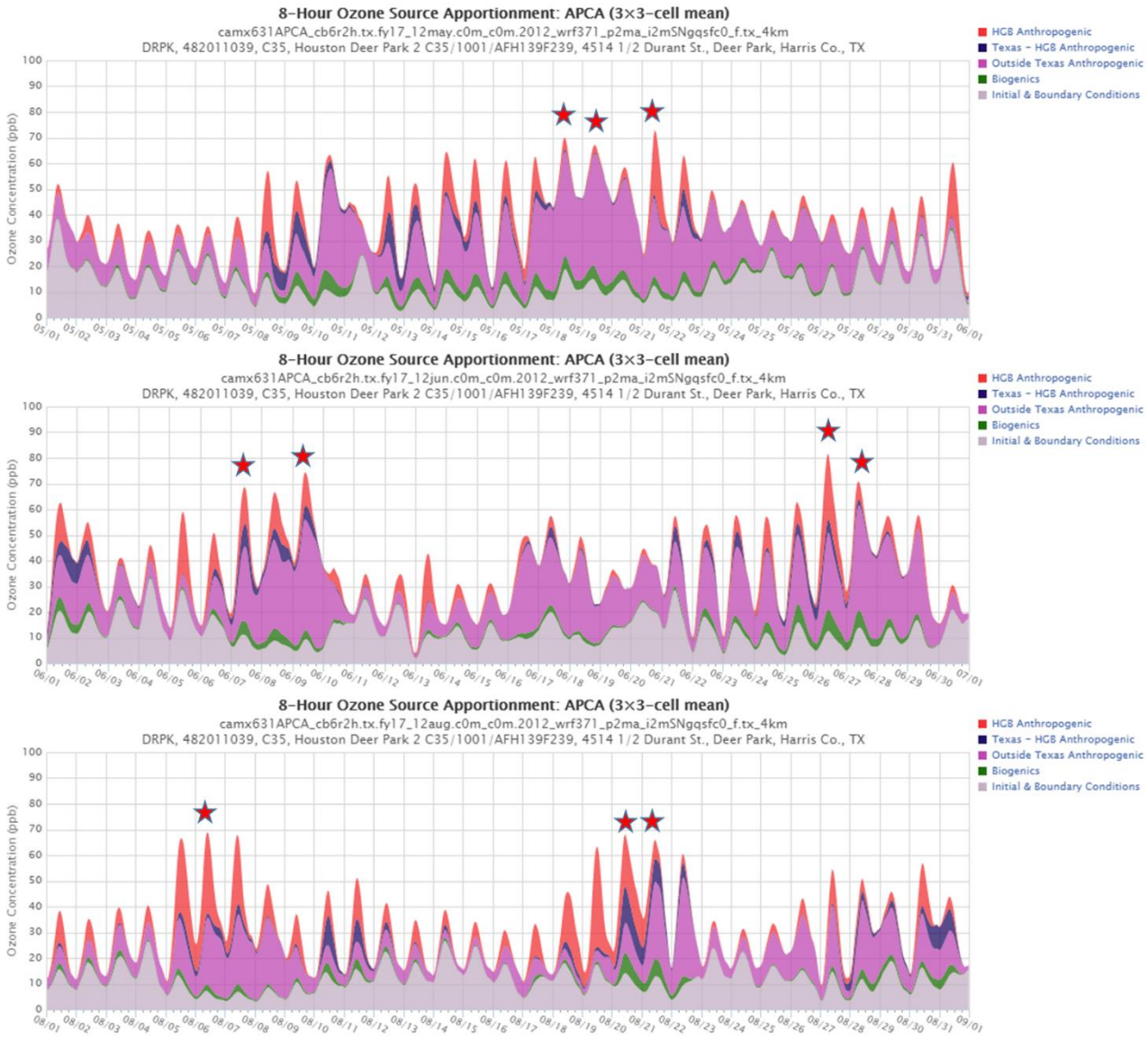

Figure 6-13: May, June, and August Modeled Future Eight-Hour Ozone Contributions by Source Region at Deer Park (C35)

Figure 6-14: *August Texas – HGB Modeled Future Eight-Hour Ozone Contributions by Source Category at Deer Park (C35)* further breaks out the Texas outside HGB contributions for August. On August 20 Texas sources outside HGB contributed a total of 14.2 ppb to the day's MDA8 ozone, with on-road and non/off-road mobile accounting for 9.6 ppb of that. Oil and gas (2.5 ppb) and Non-EGU points (1.6 ppb) also played minor roles. On August 21 the largest contributor from Texas – HGB was non-EGU point sources with 4.8 ppb, followed by on-road mobile contributing 2.8 ppb. No other sources contributed more than 0.67 ppb.

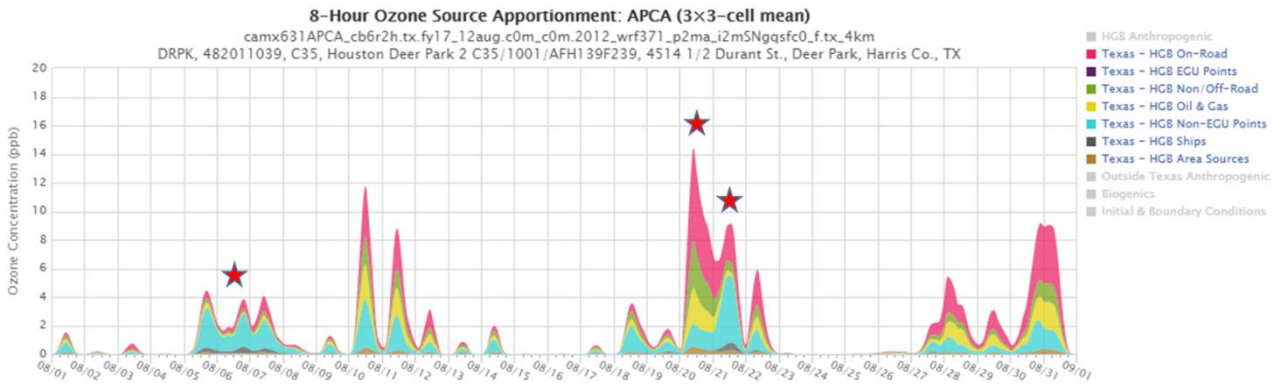

Figure 6-14: August Texas – HGB Modeled Future Eight-Hour Ozone Contributions by Source Category at Deer Park (C35)

Table 6-7: *Contributions from HGB Source Categories to Modeled Future 8-Hour Ozone for Three Selected Days at Deer Park (C35)* shows a breakdown of the local contribution to MDA8 ozone concentrations at Deer Park (C35) for the three selected days, with the largest contributions from HGB sources. This site reflects the mix of sources nearby with between 29 and 52% of locally sourced ozone attributed to non-EGU point sources, between 6 and 10% from ships, between 9 to 18% from non/off-road mobile, and between 6 and 9% attributed to EGU point sources. On-road mobile sources contributions were relatively modest, between 16 and 29% of ozone attributed to HGB sources.

Table 6-7: Contributions from HGB Source Categories to Modeled Future 8-Hour Ozone for Three Selected Days at Deer Park (C35)

Category	May 21 ppb, *% of HGB*, % of MDA8	June 26 ppb, *% of HGB*, % of MDA8	August 6 ppb, *% of HGB*, % of MDA8
HGB On-Road	7.40 29.00% 10.14%	4.10 15.68% 5.02%	4.99 15.70% 7.23%
HGB EGU Points	1.44 5.63% 1.97%	2.17 8.31% 2.66%	2.75 8.65% 3.98%
HGB Non/Off-Road	4.60 18.03% 6.31%	2.24 8.55% 2.74%	3.34 10.53% 4.85%
HGB Oil & Gas	0.16 0.64% 0.23%	0.21 0.79% 0.25%	0.44 1.38% 0.63%
HGB Non-EGU Points	7.29 28.58% 10.00%	13.60 51.97% 16.65%	14.86 46.75% 21.52%
HGB Ships	1.47 5.75% 2.01%	2.67 10.21% 3.27%	2.82 8.89% 4.09%
HGB Area Sources	3.16 12.37% 4.33%	1.17 4.49% 1.44%	2.58 8.11% 3.73%
HGB Total Contribution	25.53 100% 34.98%	26.17 100% 32.04%	31.78 100% 46.03%
MDA8	72.98	81.68	69.03

Table 6-8: *Modeled 2017 DV_F Components for Deer Park (C35) (ppb)* and Figure 6-15: *Modeled 2017 DV_F Components for Deer Park (*C35) show contributions from various regions and source categories to the modeled 2017 DV_F. Despite the heavy presence of nearby industrial sources and traffic, the largest contribution to Deer Park (C35)'s DV_F came from out-of-state with 33 ppb, compared with only 18 ppb from HGB sources.

Table 6-8: Modeled 2017 DV_F Components for Deer Park (C35) (ppb)

Category	IC/BC	Biogenics	HGB	Texas - HGB	Outside Texas	Source Category Total
On-Road			3.68	0.97	6.67	**11.32**
EGU Points			1.42	0.71	4.51	**6.64**
Non/Off Road			2.10	0.69	5.99	**8.78**
Oil & Gas			0.15	0.58	1.57	**2.30**
Non-EGU Points			7.64	1.91	6.69	**16.24**
Ships			1.62	0.17	2.11	**3.90**

Category	IC/BC	Biogenics	HGB	Texas - HGB	Outside Texas	Source Category Total
Area Sources			1.47	0.16	5.50	**7.13**
Source Region Total	**12.91**	**5.70**	**18.08**	**5.19**	**33.04**	**74.92**

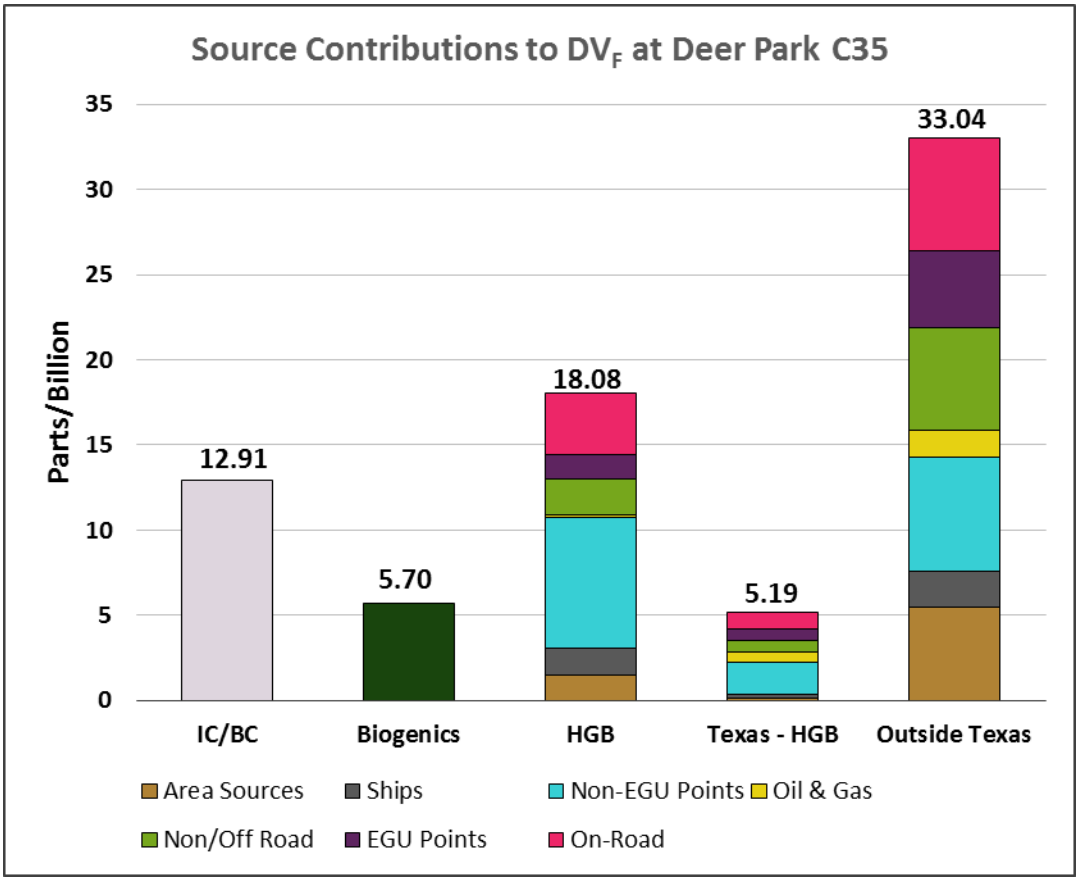

Figure 6-15: Modeled 2017 DV_F Components for Deer Park (C35)

6.5 GALVESTON (C1034)

Galveston (C1034) (refer to Figure 3-1) often benefits from very clean air off the Gulf of Mexico, particularly in the month of July, but can also receive some polluted air under northerly or easterly wind flow. Figure 6-16: *May, June, and September Modeled Future Eight-Hour Ozone Contributions by Source Region at Galveston (C1034)* shows modeled 2017 ozone for May, June, and September at Galveston (C1034), the three months having top ten MDA8 ozone concentrations. All but three selected days were strongly dominated by out-of-state pollution, though some had relatively large contributions from Texas sources outside HGB of between 5 and 8 ppb.

Some days have higher MDA8 ozone concentrations than some of the days used in calculating the DV_F. This can occur for a couple of reasons. First, because the days used in the DV_F calculation are selected using the baseline modeling, not the future case, and certain days will respond to future emission reductions better than others. Second,

the APCA source contributions are calculated as the 3x3 grid-cell average around a monitor, while the DV_F calculation is based on the 3x3 grid cell maximum as suggested in the EPA's December 2014 *Draft Modeling Guidance for Demonstrating Attainment of Air Quality Goals for Ozone, $PM_{2.5}$, and Regional Haze*. In cases where a strong concentration gradient exists, the maximum can differ substantially from the average.

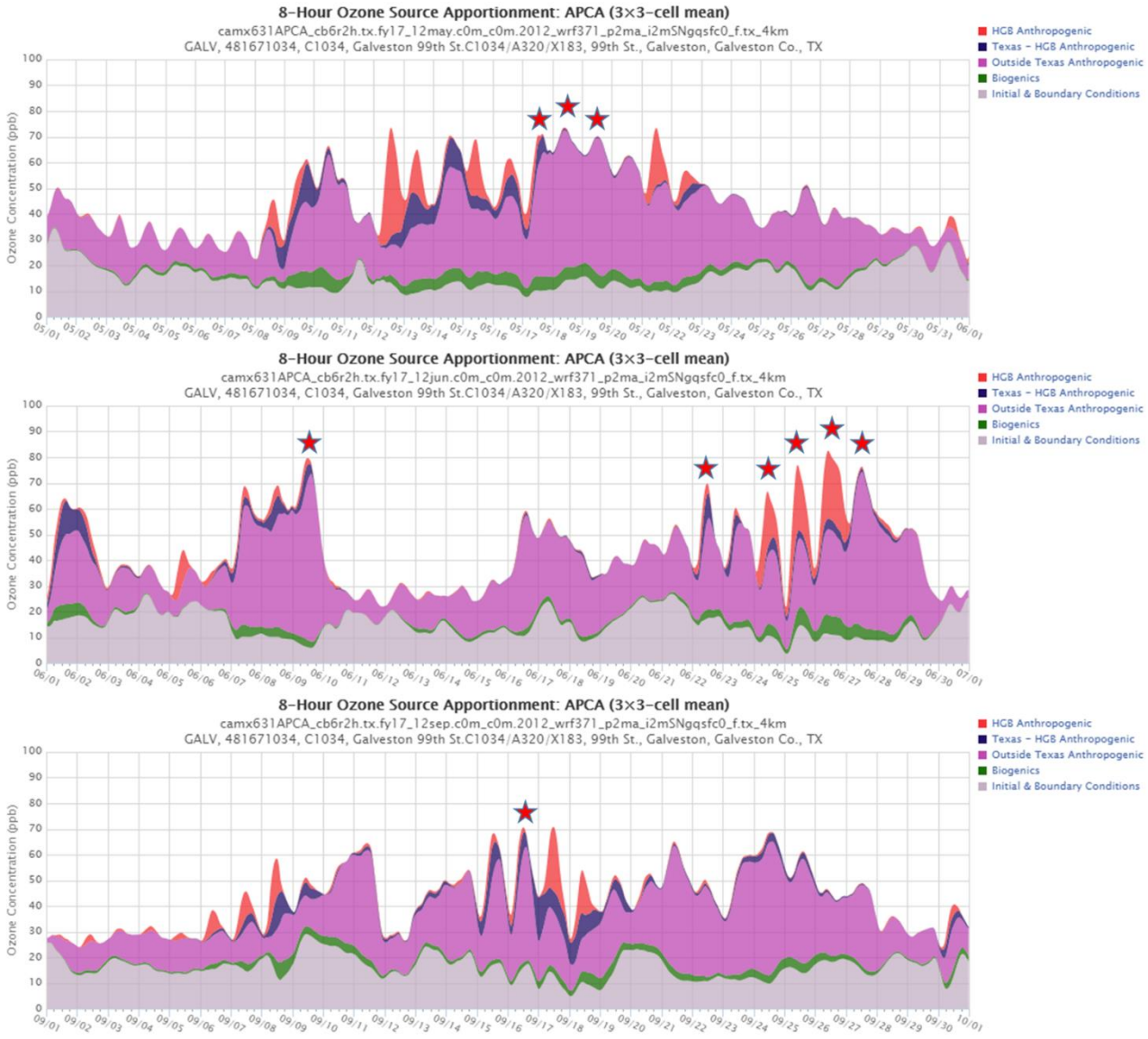

Figure 6-16: May, June, and September Modeled Future Eight-Hour Ozone Contributions by Source Region at Galveston (C1034)

Table 6-9: *Contributions from HGB Source Categories to Modeled Future Eight-Hour Ozone for Three Days at Galveston (C1034)* shows the breakdown of ozone produced by HGB sources for the three days with the largest local contributions. This site is distinguished by the large impact from shipping, ranging between 17 and 35% of total locally-produced ozone. HGB non-EGU point sources contribute between 25 and 36%, on-road mobile between 21 and 25%, and non/off-road mobile from 10 to 16%.

Table 6-9: Contributions from HGB Source Categories to Modeled Future Eight-Hour Ozone for Three Days at Galveston (C1034)

Category	**June 24 ppb**, *% of HGB*, % of MDA8	**June 25 ppb**, *% of HGB*, % of MDA8	**June 26 ppb**, *% of HGB*, % of MDA8
HGB On-Road	**5.61 ppb** *24.70%* 8.39%	**6.15 ppb** *24.10%* 8.00%	**5.50 ppb** *20.70%* 6.66%
HGB EGU Points	**0.60 ppb** *2.62%* 0.89%	**1.12 ppb** *4.39%* 1.46%	**0.54 ppb** *2.04%* 0.66%
HGB Non/Off-Road	**3.70 ppb** *16.27%* 5.53%	**3.09 ppb** *12.12%* 4.02%	**2.77 ppb** *10.45%* 3.36%
HGB Oil & Gas	**0.35 ppb** *1.52%* 0.52%	**0.28 ppb** *1.08%* 0.36%	**0.49 ppb** *1.86%* 0.60%
HGB Non-EGU Points	**6.52 ppb** *28.71%* 9.75%	**9.09 ppb** *35.62%* 11.83%	**6.56 ppb** *24.69%* 7.95%
HGB Ships	**4.86 ppb** *21.40%* 7.27%	**4.25 ppb** *16.64%* 5.52%	**9.34 ppb** *35.19%* 11.33%
HGB Area Sources	**1.09 ppb** *4.78%* 1.62%	**1.54 ppb** *6.05%* 2.01%	**1.35 ppb** *5.08%* 1.64%
HGB Total Contribution	**22.73 ppb** *100%* 33.98%	**25.52 ppb** *100%* 33.20%	**26.55 ppb** *100%* 32.19%
MDA8	**66.89 ppb**	**76.88 ppb**	**82.48 ppb**

Table 6-10: *Modeled 2017 DV_F Components for Galveston (C1034) (ppb)* and Figure 6-17: *Modeled 2017 DV_F Components for Galveston (C1034)* show contributions from various regions and source categories to the modeled 2017 DV_F. Despite the heavy presence of nearby industrial sources and traffic, the largest contribution to Deer Park's DV_F came from out-of-state.

Table 6-10: Modeled 2017 DV_F Components for Galveston (C1034) (ppb)

Category	IC/BC	Biogenics	HGB	Texas - HGB	Outside Texas	Source Category Total
On-Road			3.10	0.51	5.89	**9.50**
EGU Points			0.47	0.40	4.14	**5.01**
Non/Off Road			1.92	0.34	5.16	**7.42**
Oil & Gas			0.28	0.48	1.64	**2.40**
Non-EGU Points			4.10	2.60	6.78	**13.48**
Ships			2.60	0.32	5.17	**8.09**
Area Sources			1.15	0.13	9.10	**10.38**
Source Region Total	**10.73**	**4.13**	**13.62**	**4.78**	**37.88**	**71.14**

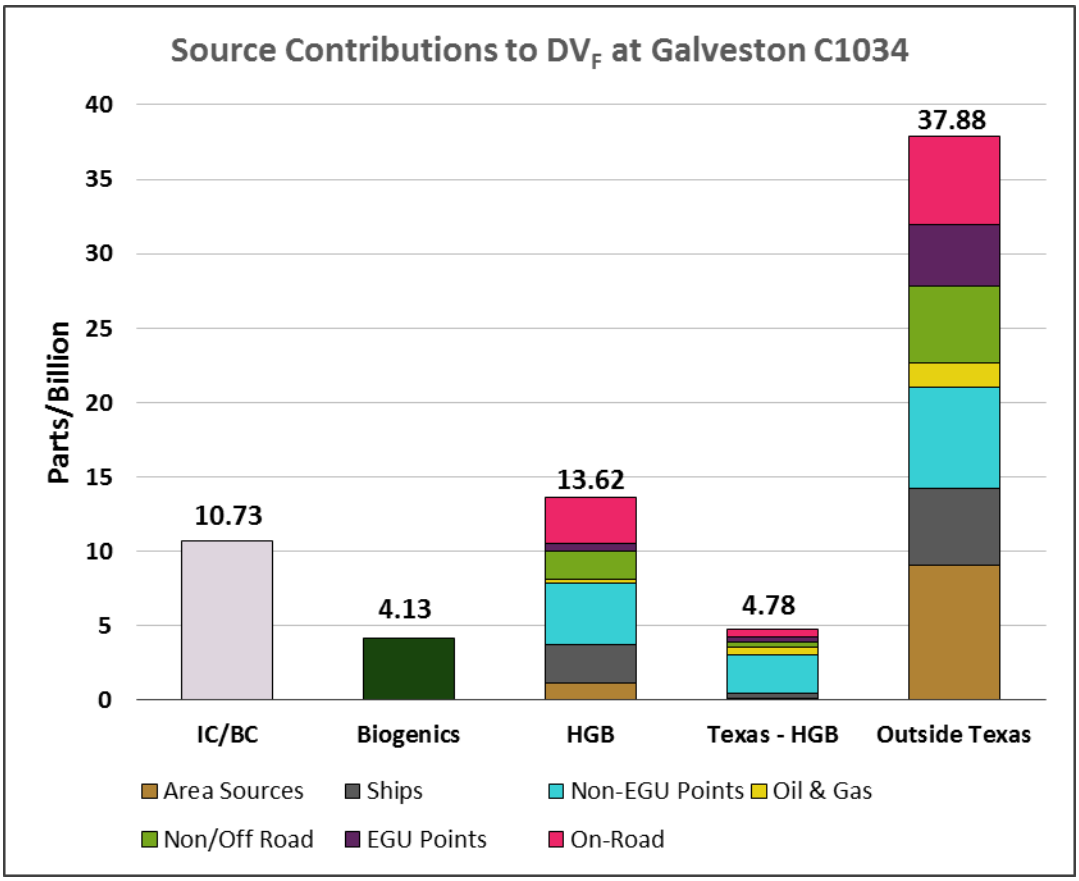

Figure 6-17: Modeled 2017 DV_F Components for Galveston (C1034)

6.6 CONROE RELOCATED (C78)

Conroe Relocated (C78) is in the north-central part of the HGB ozone nonattainment area (See Figure 3-4). Figure 6-18: *May through September Modeled Future Eight-Hour Ozone Contributions by Source Region at Conroe Relocated (C78)* shows that this site

can be strongly dominated by out-of-state sources on some days (e.g. May 18 and 19), but equally dominated by HGB sources on others (July 17).

Figure 6-18: May through September Modeled Future Eight-Hour Ozone Contributions by Source Region at Conroe Relocated (C78)

Table 6-11: *Contributions from HGB Source Categories to Modeled Future Eight-Hour Ozone for Three Days at Conroe Relocated (C78)* provides a breakdown of contributions to locally-generated ozone for three days strongly influenced by HGB sources. Despite occurring in three different months, the relative contributions of the largest contributors are remarkably consistent among the three days. The largest contributor for all three days is on-road mobile, responsible for between 34 and 37% of locally-sources ozone. Non-EGU point sources contribute 20 to 22%, and non/off-road mobile sources contribute from 18 to 22%. Area sources make a particularly large contribution at this location and have more variability than the other major contributors, ranging from 12 to 20%.

Table 6-11: Contributions from HGB Source Categories to Modeled Future Eight-Hour Ozone for Three Days at Conroe Relocated (C78)

Category	**July 17 ppb**, *% of HGB*, % of MDA8	**August 7 ppb**, *% of HGB*, % of MDA8	**September 24 ppb**, *% of HGB*, % of MDA8
HGB On-Road	**12.25 ppb** *34.10%* *20.97%*	**10.33 ppb** *36.89%* 16.80%	**8.24 ppb** *35.21%* 11.22%
HGB EGU Points	**0.84 ppb** *2.35%* 1.44%	**1.84 ppb** *6.56%* 2.99%	**0.63 ppb** *2.69%* 0.86%
HGB Non/Off-Road	**6.64 ppb** *18.48%* 11.36%	**5.02 ppb** *17.94%* 8.17%	**5.10 ppb** *21.80%* 6.95%
HGB Oil & Gas	**0.38 ppb** *1.07%* 0.66%	**0.44 ppb** *1.56%* 0.71%	**0.22 ppb** *0.93%* 0.30%
HGB Non-EGU Points	**7.73 ppb** *21.52%* 13.24%	**6.17 ppb** *22.03%* 10.04%	**4.71 ppb** *20.14%* 6.42%
HGB Ships	**1.06 ppb** *2.96%* 1.82%	**0.93 ppb** *3.32%* 1.51%	**0.83 ppb** *3.54%* 1.13%
HGB Area Sources	**7.01 ppb** *19.52%* 12.01%	**3.28 ppb** *11.71%* 5.33%	**3.67 ppb** *15.69%* 5.00%
HGB Total Contribution	**35.92 ppb** *100%* 61.50%	**28.00 ppb** *100%* 45.55%	**23.40 ppb** *100%* 31.86%
MDA8	**58.40**	**61.47**	**73.43**

The breakout of sources contributing to the design value at Conroe Relocated in Table 6-12: *Modeled 2017 DV_F Components for Conroe Relocated (C78) (ppb)* and Figure 6-19: *Modeled 2017 DV_F Components for Conroe Relocated (C78)* shows that sources outside

Texas contribute more to the site's DV_F than all anthropogenic Texas sources, both inside and out of HGB.

Table 6-12: Modeled 2017 DV_F Components for Conroe Relocated (C78) (ppb)

Category	IC/BC	Biogenics	HGB	Texas - HGB	Outside Texas	Source Category Total
On-Road			7.52	0.62	5.02	**13.16**
EGU Points			0.83	0.51	3.42	**4.76**
Non/Off Road			4.11	0.43	4.40	**8.94**
Oil & Gas			0.19	0.43	1.25	**1.87**
Non-EGU Points			4.37	1.27	5.68	**11.32**
Ships			0.83	0.11	2.37	**3.31**
Area Sources			2.83	0.11	5.30	**8.24**
Source Region Total	**17.32**	**4.14**	**20.68**	**3.48**	**27.44**	**73.06**

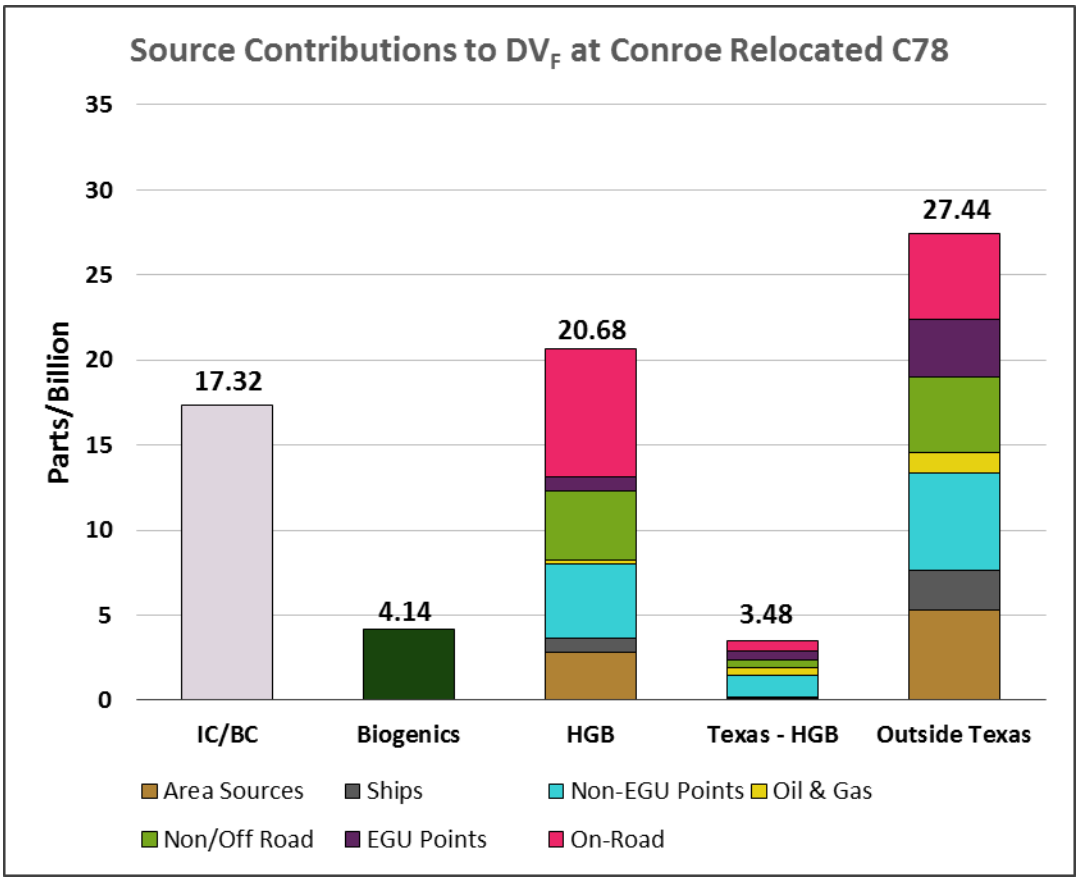

Figure 6-19: Modeled 2017 DV_F Components for Conroe Relocated (C78)

6.7 DISCUSSION

The contributions to ozone in the HGB area vary significantly from monitor to monitor, but all showed a large influence from sources outside Texas on many days, both high and low ozone. At each site studied, however, HGB sources became a dominant influence on MDA8 ozone on at least a few high-ozone days. Initial and boundary conditions contributed between 10 and 12 ppb to the ozone DV_F except at Conroe Relocated C78, where the model attributed 17 ppb to IC/BC. Biogenics contributed 4 to 6 ppb at each site studied.

Sources in Texas but outside HGB played a minor role for most sites and days, but did contribute substantially on occasion.

Of HGB sources, on-road mobile was the largest contributor to 2017 DV_F at Conroe Relocated (C78), Aldine (C8), and Manvel Croix Park (C84), while non-EGU point sources had the largest contribution to Galveston (C1034) and Deer Park (C35). Sites were also affected differentially by local sources; for example, ships were minor contributors at sites except Galveston (C1034) and Deer Park (C35), while area sources were more important at Aldine (C8), Manvel Croix Park (C84), and Conroe Relocated (C78).

At the Manvel Croix Park (C84) monitor, the modeling indicated that anthropogenic NO_X is responsible for the major share of modeled 2017 MDA8 ozone, although VOC does account for a few ppb.